NATIONAL ADVISORY COMMITTEE FOR AERONAUTICS

TECHNICAL NOTE

NO. 1554

APPLICATION OF THE LINEARIZED THEORY OF SUPERSONIC FLOW TO THE ESTIMATION OF CONTROL-SURFACE CHARACTERISTICS

By Charles W. Frick, Jr.

Ames Aeronautical Laboratory
Moffett Field, Calif.

Washington
March 1948

NATIONAL ADVISORY COMMITTEE FOR AERONAUTICS

TECHNICAL NOTE NO. 1554

APPLICATION OF THE LINEARIZED THEORY OF SUPERSONIC FLOW TO THE ESTIMATION OF CONTROL-SURFACE CHARACTERISTICS

By Charles W. Frick, Jr.

SUMMARY

Known conical-flow solutions of the linearized equation for the velocity potential in supersonic flow are applied to the calculation of the characteristics of control surfaces. Complete solutions for the pressure distributions are obtained for control surfaces with hinge lines swept ahead of or behind the Mach line when the control-surface trailing edge is swept ahead of the Mach line. Useful approximate solutions of good accuracy are obtained when the trailing edge is swept behind the Mach line. Applications of the theory to the estimation of the hinge-moment and effectiveness characteristics of elevators and ailerons are presented.

INTRODUCTION

While the characteristics of control surfaces are influenced to a large extent by viscosity effects so that extensive experimental investigations are required, it is evident that theoretical estimations of these characteristics are necessary for coordinated experiments. Existing theoretical treatments consider, for the most part, cases where the hinge line and trailing edge are swept ahead of the Mach lines and special control types.[1]

In the present report, control surfaces with hinge lines swept ahead of or behind the Mach line[2] and with trailing edges swept ahead of or behind the Mach line are considered. Use is made of the solution for line sources in the acceleration potential field as given by

---

[1]Notably in a paper by P.A. Lagerstrom given at the winter meeting of the Institute of the Aeronautical Sciences in New York City, January 27 - 30, 1948.

[2]It has been found convenient to designate a hinge line swept ahead of or behind the Mach line as a supersonic or a subsonic hinge line. This notation is also applied to trailing and leading edges and always means that the component of the stream velocity perpendicular to the line or edge referred to is supersonic or subsonic.

R. T. Jones in reference 1 to determine the basic lift[3] due to control-surface deflection. The effects of the interaction between the upper and lower surfaces around the subsonic edges of the plan form are determined by a "cancellation of lift" method originated by Dr. Paco Lagerstrom and used by him in a recent paper treating downwash calculations presented before the 1947 summer meeting of the Institute of Aeronautical Sciences in Los Angeles. This method was subsequently applied by Doris Cohen in a recent NACA report (reference 2) to the calculation of the characteristics of flat lifting wings at supersonic speeds. The notation of reference 2 is used throughout this report.

SYMBOLS AND COEFFICIENTS

x,y,z	Cartesian coordinates
V	flight velocity
M	Mach number
β	$\sqrt{M^2-1}$
u	perturbation velocity in x-direction
q	dynamic pressure $\left(\frac{1}{2}\rho V^2\right)$
$\frac{\Delta p}{q}$	lifting-pressure coefficient
δ	angular deflection of the control surface about the hinge line, downward movement of the trailing edge considered positive deflection
s	value of y defining distance from origin of coordinates to the tip of the wing
b	span of the wing

[3]Throughout this report, the term "basic lift" means the lift provided by the deflection of the control surface without consideration of the induced negative lift due to the interaction between the upper and lower surfaces of the wing around the subsonic edges of the plan form.

b_1 spanwise distance from wing center line to inboard end of aileron

a parameter defining a ray from the origin[4] $\left(a = \frac{\beta y}{x}\right)$

a_t value of a for the ray from the origin which passes through the trailing edge of the tip of the wing[4]

a_l the value of a for the ray that passes through the leading edge of the tip of the wing[4]

m β times inclination of the hinge line (the value of a for the ray which lies along the hinge line)[4]

m_t β times inclination of the trailing edge measured from the x-axis[4]

m_l β times inclination of the wing leading edge measured from the x-axis[4]

t_a parameter defining a ray from the apex of a superposed sector $\left[t_a = \frac{\beta(y-y_a)}{x-x_a}\right]$

y_a value of y at the apex of any superposed constant lift sector

x_a value of x at the apex of any superposed constant lift sector

c_o chord of the control surface along the x-axis

$\bar{c}$ root mean square chord of the control surface

c_w chord of the wing (including the control surface) at the origin of coordinates measured in the x-direction

c_a mean aerodynamic chord of the wing

X distance from the vertex of the wing to the origin of coordinate of the control surface in the x-direction

S wing area

L lift or rolling moment

[4]As shown in figure 1.

M pitching moment

H hinge moment

C_{l_p} damping in roll

$\frac{pb}{2V}$ wing-tip helix angle

C_{h_δ} variation of hinge-moment coefficient with control-surface deflection at constant wing angle of attack

C_{h_α} variation of hinge-moment coefficient with wing angle of attack at constant control deflection

C_{L_δ} variation of lift coefficient with deflection of control surface at constant wing angle of attack

C_{L_α} variation of lift coefficient with wing angle of attack at constant control-surface deflection

C_{n_δ} variation of yawing-moment coefficient with control-surface deflection at constant angle of attack

α_δ ratio of the angle of attack necessary to produce unit lift coefficient at constant control deflection to the control deflection necessary to produce unit lift coefficient at constant wing angle of attack $(-C_{L_\delta}/C_{L_\alpha})$

C_{m_δ} variation of pitching-moment coefficient with control-surface deflection at constant wing angle of attack

C_{l_δ} variation of rolling-moment coefficient with control-surface deflection at constant sideslip angle

BASIC LIFT DISTRIBUTION DUE TO CONTROL-SURFACE DEFLECTION

For the purpose of obtaining the lift produced by and the hinge moment resulting from the deflection of a thin flat control surface hinged on a thin flat wing, it may be assumed that within the limitations of the linear theory, the lift produced by control-surface deflection is independent of the lift produced by the angle of attack of the wing. This assumption eliminates the necessity of considering the wing plan form except within the zone of influence of the control surface and permits the application of known

linearized mathematical solutions for supersonic flow.[5]

In developing the linear theory of control surfaces at supersonic speeds, it is convenient to divide the total lift provided by the deflection of the control surface hinged on a finite wing into two parts. The first part, which will be called the basic lift, is the lift provided by the deflection of the control surface when the wing boundaries extend to the Mach cone in the cross-stream direction and to infinity in the downstream direction or in other words when the extent of the wing is such as to preclude interaction between the upper and lower surfaces. The second part, known as the induced lift, is the lift, usually negative, which is due to the interaction between the upper and lower surfaces around the subsonic edges of the wing plan form.

The origin of the coordinate system is placed at the foremost point of the hinge line of the control surface as shown in figure 1. It is found that the following boundary conditions must be satisfied in the mathematical treatment of the basic lift.

(a) The surface behind the hinge line must be flat and have the slope in the stream direction

$$\frac{dz}{dx} = \delta \cos \cot^{-1} \frac{m}{\beta} = \delta \frac{m}{\sqrt{\beta^2+m^2}}$$

(b) The surface ahead of the hinge line must be flat and must extend up to or forward of the Mach cone from the origin; in other words, no downwash or upwash due to control deflection may exist ahead of the hinge line.

The solution corresponding to these boundary conditions is that for an inclined line source in the acceleration potential field given by R. T. Jones in reference 1. The line source results in a wedge-shaped figure, of course, but for the purpose of treating control surfaces the velocity distribution on only one side of the wedge need be considered, since no interaction between upper and lower surfaces

[5] It should be noted that the deflection of a control surface produces a gap between the control surface and the adjacent wing surface through which a leakage of air may take place. Leakage may also occur from the lower to the upper surface of the wing if the gap at the hinge line is unsealed. The effect of leakage cannot be determined theoretically because of viscosity effects. An experimental investigation is required.

exists. The perturbation velocities are equal on both upper and lower surfaces of the control surface but are of opposite sign so that the lifting-pressure coefficient is

$$\frac{\Delta p}{q} = 4 \frac{u}{V}$$

When the results of reference 1 are applied to a control surface with the hinge line swept behind the Mach cone from the origin (a subsonic hinge line), it is found that the lifting-pressure coefficient is given by

$$\frac{\Delta p}{q} = \frac{4}{\pi} \frac{\delta}{\beta} \frac{m^2}{\sqrt{(\beta^2+m^2)(1-m^2)}} \cosh^{-1} \frac{(1-ma)}{|a-m|} \tag{1}$$

where $a = \frac{\beta y}{x}$, defining any ray from the origin. ($|a-m|$ indicates absolute value is to be used.)

If the hinge line is swept ahead of the Mach cone

$$\frac{\Delta p}{q} = \frac{4}{\pi} \frac{\delta}{\beta} \frac{m^2}{\sqrt{(\beta^2+m^2)(m^2-1)}} \cos^{-1} \frac{(1-ma)}{|a-m|} \tag{2}$$

These equations give the lifting-pressure coefficient for any point within the zone of influence of the control surface including that portion of the wing adjacent to the inboard end of the control surface. Figure 2 shows typical pressure distributions.

If equations (1) and (2) are rewritten as

$$\frac{\Delta p}{q} = \frac{4}{\pi} \frac{\delta}{\beta} \frac{m^2}{\sqrt{(\beta^2+m^2)(1-m^2)}} G(a) \tag{3}$$

and

$$\frac{\Delta p}{q} = \frac{4}{\pi} \frac{\delta}{\beta} \frac{m^2}{\sqrt{(\beta^2+m^2)(m^2-1)}} F(a) \tag{4}$$

the basic lifting-pressure coefficients for a variety of control-surface configurations can be expressed. Thus, for a single control

surface similar to the aileron of figure 1(a)

$$G(a) = \cosh^{-1}\frac{1-ma}{|a-m|}$$

and

$$F(a) = \cos^{-1}\frac{1-ma}{|a-m|}$$

For two adjacent control surfaces deflected equal amounts, such as the elevators of figure 1(b)

$$G(a) = \cosh^{-1}\frac{1-ma}{|a-m|} + \cosh^{-1}\frac{1+ma}{|a+m|}$$

and

$$F(a) = \cos^{-1}\frac{1-ma}{|a-m|} + \cos^{-1}\frac{1+ma}{|a+m|}$$

If the adjacent control surfaces are equally deflected but in opposite directions such as to produce a rolling moment

$$G(a) = \cosh^{-1}\frac{1-ma}{|a-m|} - \cosh^{-1}\frac{1+ma}{|a-m|}$$

and

$$F(a) = \cos^{-1}\frac{1-ma}{|a-m|} - \cos^{-1}\frac{1+ma}{|a+m|}$$

Unequal deflections can, of course, be treated by inserting proportionality factors as coefficients for the terms in the expressions for $G(a)$ and $F(a)$. If the control surfaces are not adjacent but have overlapping zones of influence, separate origins are selected for each.

If the control surface does not extend to the tip of the wing,

$$G(a) = \cosh^{-1}\frac{1-ma}{|a-m|} - \cosh^{-1}\frac{1-ma_b}{|a_b-m|}$$

and

$$F(a) = \cos^{-1}\frac{1-ma}{|a-m|} - \cos^{-1}\frac{1-ma_b}{|a_b-m|}$$

where a_b is referred to the outboard end of the hinge line as origin.

$$a_b = \frac{y-y_b}{x-x_b}$$

Here x_b and y_b are the coordinates of the outboard end of the hinge line.

The second term in the expression for $G(a)$ in this case corresponds to the superposition of a line sink along the hinge line with its origin at x_b,y_b canceling the deflection of the control surface beyond this point.

INDUCED LIFT

The basic lift produced by the deflection of a control surface has been shown to be given by rather simple mathematical expressions. In order to complete the calculation of the pressures due to control-surface deflection, it is necessary to determine the effects of the interaction between the upper and lower surfaces of the wing around the subsonic edges of the plan form which fall within the zone of influence of the control surface. Since the pressure field due to the basic lift is conical in form, the powerful method of the superposition of constant-lift sectors used in reference 2 is readily applicable to the calculation of these induction effects. In the following treatment, the incremental pressures determined by this method are to be added algebraically to the basic lifting pressures to obtain a complete solution.

Tip

When the tip is alined with the stream, it is evident that interaction between the upper and lower surfaces of the control surface exists within the Mach cone with its apex at the point where the Mach cone of the control surface intersects the tip. The extent of the induced negative lift resulting from the interaction may be determined in the following manner.

The pressure difference that exists along the tip due to the basic lift is canceled by the integrated effect of the superposition of triangular elements of constant lift as shown in figure 3(a). The sectors are so placed that one edge is along the tip and the

other along a ray a from the origin. The characteristics of these sectors are such that between the edge along the tip and the Mach cone from the apex of the sector – the region overlapping the wing – no downwash exists, so that the shape of the control surface remains unaltered after superposition. In this same region, the lifting-pressure coefficient is variable. Between the edge along the tip and the edge along the ray a the lifting-pressure coefficient is constant and the downwash variable. Between the edge along the ray a and the sector Mach cone, the lifting-pressure coefficient is zero.

The distribution of the lifting-pressure coefficient for the superposed sector for all regions is given by reference 2 as[6]

$$\left(\frac{\Delta p}{q}\right)_{\substack{\text{tip}\\ \text{sector}}} = \left(\frac{\Delta p}{q}\right)_a \left(\frac{1}{\pi}\cos^{-1}\frac{a+t_a+2at_a}{t_a-a}\right)$$

where t_a defines a ray from the apex of the sector passing through the point x,y under consideration and $(\Delta p/q)_a$ is the magnitude of the constant-pressure coefficients over the sector.

If $(\Delta p/q)_a$ is given the value $\frac{d}{da}\left(\frac{\Delta p}{q}\right)da$, that is, the rate of change of the basic-pressure coefficient with a times da, then the induced pressure coefficient at any point x,y due to the superposition of the sectors along the tip is given by

$$\Delta\left(\frac{\Delta p}{q}\right)_{tip} = -\frac{1}{\pi}\int \frac{d}{da}\left(\frac{\Delta p}{q}\right)\cos^{-1}\frac{a+t_a+2at_a}{t_a-a}\,da$$

For a control surface with a subsonic hinge line

$$\Delta\left(\frac{\Delta p}{q}\right)_{tip} = -\frac{4}{\pi^2}\frac{\delta}{\beta}\frac{m^2}{\sqrt{(\beta^2+m^2)(1-m^2)}}\int_1^{a_o} G'(a)\cos^{-1}\frac{a+t_a+2at_a}{t_a-a}\,da \quad (5)$$

where

$$t_a = \beta\frac{(y-s)}{x-\frac{\beta s}{a}}$$

[6] The functions describing the pressure-coefficient distribution for this sector and the other sectors given herein are those applied to the right-hand side of the wing where y is positive.

and $G'(a)$ is the derivative with respect to a of the $G(a)$ term of equation (3). The integration must be performed from the Mach cone, where $G(a)$ is zero, back to the value of a, a_o, for which the Mach cone from the vertex of the triangular sector x_a, s passes through the point x,y under consideration. For the tip,

$$a_o = \frac{\beta s}{x+\beta(y-s)}$$

Although the value of $G'(a)$ becomes infinite at $a=1$ and $a=m$, the integral is finite and may be evaluated by graphical means. (See Appendix A.)

If the Mach cone of the control surface sweeps over the leading edge of the wing to which the control surface is attached as shown in figure 1(a), equation (5) is modified as follows

$$\Delta\left(\frac{\Delta p}{q}\right)_{tip} = -\frac{4}{\pi^2}\frac{\delta}{\beta}\frac{m^2}{\sqrt{(\beta^2+m^2)(1-m^2)}}\left[G(a_l)\cos^{-1}\frac{a_l+t_{a_l}+2a_l t_{a_l}}{t_{a_l}-a_l} + \int_{a_l}^{a_o} G'(a)\cos^{-1}\frac{a+t_a+2at_a}{t_a-a}\,da\right] \tag{5a}$$

where $G(a_l)$ is the value of the term $G(a)$ at $a=a_l$ and t_{a_l} denotes a ray from the sector superposed with its apex at the leading edge of the tip.

For a control surface with the hinge line swept ahead of the Mach cone from the origin the solution for the tip interaction effects is as follows:

$$\Delta\left(\frac{\Delta p}{q}\right)_{tip} = -\frac{4}{\pi^2}\frac{\delta}{\beta}\frac{m^2}{\sqrt{(\beta^2+m^2)(m^2-1)}}\left[\pi\cos^{-1}\frac{m+t_m+2mt_m}{t_m-m} - \int_1^{a_o} F'(a)\cos^{-1}\frac{a+t_a+2at_a}{t_a-a}\,da\right] \tag{6}$$

where t_m is the value of t_a when $a=m$ and $F'(a)$ is the derivative with respect to a of the $F(a)$ term of equation (4).

The integration again must be carried to a_o and may be evaluated graphically. (See Appendix A.)

Effect of Trailing Edge

If the trailing edge of the control surface is supersonic, superposition of constant-lift sectors along the trailing edge to cancel the lift in the stream due to the hinge-line source does not influence the pressures ahead of the trailing edge. In this case only the induced lift in the tip region needs be considered.

When the trailing edge of the control surface is subsonic, interaction will exist between the upper and lower surfaces. The lift must fall to zero at the trailing edge, that is, the Kutta condition must be met. The methods of reference 2 may also be used in this case to evaluate the induced lift. Again the superposition of constant-lift sectors with one edge along the trailing edge and one edge along a ray a is used. The sectors have been so derived (fig. 3(b)) that there is zero downwash between the right sector Mach line and the edge of the sector along the trailing edge - the region overlapping the wing - and zero lift between the edge of the sector along the ray a and the left sector Mach line. The distribution of lifting-pressure coefficient within the Mach cone of the superposed sector is given by reference 2 as

$$\left(\frac{\Delta p}{q}\right)_{\text{oblique sector}} = \left(\frac{\Delta p}{q}\right)_a \frac{1}{\pi} \cos^{-1} \frac{(1+m_t)(a+t_a)-2(at_a+m_t)}{(1-m_t)(t_a-a)}$$

where $(\Delta p/q)_a$ is the magnitude of the constant-pressure coefficient, and t_a defines a ray from the apex of the sector.

For a single control surface such as the aileron of figure 1, the induced pressures are obtained again by setting $(\Delta p/q)_a$ equal to the rate of change of the basic lift with a times da.

For a subsonic hinge line

$$\Delta\left(\frac{\Delta p}{q}\right)_{TE} = -\frac{4}{\pi^2}\frac{\delta}{\beta}\frac{m^2}{\sqrt{(\beta^2+m^2)(1-m^2)}}\int_{-1}^{a_o} G'(a) \cos^{-1}\frac{(1+m_t)(a+t_a)-2(at_a+m_t)}{(1-m_t)(t_a-a)}\,da \qquad (7)$$

and for a supersonic hinge line

$$\Delta\left(\frac{\Delta p}{q}\right)_{TE} = -\frac{4}{\pi^2}\frac{\delta}{\beta}\frac{m^2}{\sqrt{(\beta^2+m^2)(m^2-1)}}\int_{-1}^{a_o} F'(a)\cos^{-1}\frac{(1+m_t)(a+t_a)-2(at_a+m_t)}{(1-m_t)(t_a-a)}\,da \tag{8}$$

In these equations, t_a defines a ray from the vertex of any constant-lift sector passing through the point x,y under consideration

$$t_a = \frac{\beta y(m_t-a)-m_t c_o a}{x(m_t-a)-m_t c_o}$$

The integrations shown must be carried out from the Mach cone, $a = -1$ to the value of a, a_o, corresponding to the last superposed sector the Mach cone of which passes through the point x,y under consideration.

For the trailing-edge correction,

$$a_o = m_t\frac{\beta y+c_o-x}{\beta y+c_o m_t-x}$$

For adjacent control surfaces similar to the elevators of figure 1(b), the finite lifting pressure along the ray $a=0$ is canceled by use of a symmetrical constant-load triangle with its apex at $c_o,0$ (fig. 3(c)) which has no downwash or upwash between the leading edge and the Mach cone. The pressure field of the triangle is given by reference 2 as

$$\frac{\Delta p}{q} = \left(\frac{\Delta p}{q}\right)_{a=0}\frac{1}{\pi}\cos^{-1}\frac{(1+m_t^2)t_o^2-2m_t^2}{(1-m_t^2)t_o^2}$$

where $(\Delta p/q)_{a=0}$ is the lifting-pressure coefficient due to the hinge-line sources along ray a=0. In this equation, t_o defines a ray from the vertex of the triangle at $c_o,0$, through x,y.

$$t_o = \frac{\beta y}{x-c_o}$$

The remaining lift along the trailing edge is canceled in the same manner as for the previous case so that for a subsonic hinge line, the total induced pressure coefficient is given by

$$\Delta\left(\frac{\Delta p}{q}\right)_{TE} = -\frac{4}{\pi^2}\frac{\delta}{\beta}\frac{m^2}{\sqrt{(\beta^2+m^2)(1-m^2)}}\left[\left(2\cosh^{-1}\frac{1}{m}\right)\cos^{-1}\frac{(1+m_t^2)t_o^2-2m_t^2}{(1-m_t^2)t_o^2}\right.$$

$$\left.+\int_o^{a_o} G'(a)\cos^{-1}\frac{(1+m_t)(a+t_a)-2(at_a+m_t)}{(1-m_t)(t_a-a)}\,da\right] \tag{9}$$

and for a supersonic hinge line and subsonic trailing edge

$$\Delta\left(\frac{\Delta p}{q}\right)_{TE} = -\frac{4}{\pi^2}\frac{\delta}{\beta}\frac{m^2}{\sqrt{(\beta^2+m^2)(m^2-1)}}\left[\left(2\cos^{-1}\frac{1}{m}\right)\cos^{-1}\frac{(1+m_t^2)t_o^2-2m_t^2}{(1-m_t^2)t_o^2}\right.$$

$$\left.+\int_o^{a_o} F'(a)\cos^{-1}\frac{(1+m_t)(a+t_a)-2(at_a+m_t)}{(1-m_t)(t_a-a)}\,da\right] \tag{10}$$

The limit a_o is as defined for equations (7) and (8).

It can be seen that the pressure increments resulting from the evaluation of the interaction around the trailing edge cause negative lift to exist along and outboard of the tip within the Mach cone from the root trailing edge of the control surface. Since the pressure difference at the tip

must be zero, an additional correction must be applied to this portion of the tip. The correction is difficult since the residual-flow field is nonconical in form. This is especially true of a control surface similar to the aileron of figure 1(a) where all of the pressure induced along and outboard of the tip is due to the integrated effect of the oblique sectors placed along the trailing edge. An approximate solution may be obtained either by assuming that the pressure field at the tip resulting from the trailing-edge correction is conical from the intersection of the control-surface Mach cone and the trailing edge, or by replacing the trailing-edge basic-pressure distribution by a step distribution, a conical flow field at the tip being calculated for each trailing-edge oblique sector placed at a step.

For control surfaces similar to the elevators of figure 1(b), the correction for the lift induced beyond the tip is simplified in most cases, since the contribution of the integration of the oblique sectors along the trailing edge may be neglected. This leaves only the conical flow field due to the first term of equations (9) or (10) which may be treated in the same manner as the usual tip correction.

In like manner, the computations of tip effect are found to give a decrement in pressure along the trailing edge which is not taken into account by the trailing-edge computations mentioned previously. This flow field is also nonconical in form.

A similar situation exists because of the tip correction due to the trailing-edge influence mentioned previously. In general, it is not considered worthwhile to complete the solution of these reflected regions beyond the first one or two steps since the residual pressures are small.

Effect of Leading Edge

If the Mach cone from the origin crosses the leading edge of the wing to which the control surface is attached, the interaction between upper and lower surface may be determined again by the superposition of constant lift sectors as shown in figure 3(d). Again the sector is selected to give no downwash on the wing and constant pressure between the wing leading edge and the ray a.

The solution for such a sector has been taken from an as yet unpublished report by Dr. Paco Lagerstrom which considers many types of "mixed flow" wings. The pressure field is of the form

$$\left(\frac{\Delta p}{q}\right)_{LE\ sector} = \left(\frac{\Delta p}{q}\right)_a \frac{1}{\pi}\left[\cos^{-1}\frac{(1-m_l)(a+t_a)+2(at_a-m_l)}{(1+m_l)(t_a-a)} - \frac{2m_l}{a(1+m_l)}\sqrt{\frac{(a-m_l)(1+a)(1+t_a)}{m_l-t_a}}\right]$$

where $(\Delta p/q)_a$ is the magnitude of the constant-pressure coefficient.

It may be noted that the second term of this expression causes the local pressures to become infinite at the leading edge, an expected result of the upwash between the leading edge of the wing and the control-surface Mach cone.

Setting $\left(\frac{\Delta p}{q}\right)_a$ equal to the rate of change of the basic lift with a times da,

$$\Delta\left(\frac{\Delta p}{q}\right)_{LE} = \frac{4}{\pi^2}\frac{\delta}{\beta}\frac{m^2}{\sqrt{(\beta^2+m^2)(1-m^2)}}\left[\int_1^{a_o} G'(a)\cos^{-1}\frac{(1-m_l)(a+t_a)+2(at_a-m_l)}{(1+m_l)(t_a-a)}\,da\right.$$

$$\left. - \frac{2m_l}{1+m_l}\int_1^{a_o}\frac{G'(a)}{a}\sqrt{\frac{(a-m_l)(1+a)(1+t_a)}{m_l-t_a}}\right]$$

where

$$t_a = \frac{\beta y(a-m_l)-am_l(c_w-c_o)}{x(a-m_l)-m_l(c_w-c_o)}$$

The superposition described by this equation cancels all the lift due to control deflection ahead of the leading edge of the wing, including the lift beyond the wing tip ahead of the projected leading edge. Examination of equation 5(b) shows that the superposition of the tip sectors also cancels the lift beyond the tip in the region between the projected leading edge and the ray a_l passing through the leading edge of the tip. In this region then the cancellation of lift is duplicated. This duplication may be avoided by changing the equation for the superposition of leading-edge sectors so that the pressures ahead of the projected leading edge

outboard of the tip are not canceled by the leading-edge correction. The equation for the leading-edge induced pressures then becomes

$$\Delta\left(\frac{\Delta p}{q}\right)_{LE} = -\frac{4}{\pi^2}\frac{\delta}{\beta}\frac{m^2}{\sqrt{(\beta^2+m^2)(1-m^2)}}\left[\int_1^{a_l} G'(a)\cos^{-1}\frac{(1-m_l)(a+t_a)+2(at_a-m_l)}{(1+m_l)(t_a-a)}\,da\right.$$

$$-\frac{2m_l}{1+m_l}\int_1^{a_l}\frac{G'(a)}{a}\sqrt{\frac{(a-m_l)(1+a)(1+t_a)}{m_l-t_a}}\,da$$

$$-G(a)_l\cos^{-1}\frac{(1-m_l)(a_l-t_{a_l})+2(a_lt_{a_l}-m_l)}{(1+m_l)(t_{a_l}-a_l)}$$

$$\left.+\frac{2m_l}{1+m_l}\frac{G(a_l)}{a_l}\sqrt{\frac{(a_l-m_l)(1+a_l)(1+t_{a_l})}{m_l-t_{a_l}}}\right] \qquad (11)$$

where $G(a_l)$ is the value of $G(a)$ at $a=a_l$ and t_{a_l} denotes a ray from the apex of the sector superposed at the leading edge of the tip.

The integrations must be carried from the Mach cone, $a=1$, where $G(a)$ is zero to the leading edge of the tip $a=a_l$ unless the point x,y under consideration lies ahead of the Mach line from the tip. In this case, the integration must be carried out to a value of a, a_o, corresponding to the last superposed sector the Mach cone of which includes the point x,y. The last two terms of equation (11) disappear.

The limit a_l is given as

$$a_l = \frac{\beta s}{\frac{\beta s}{m_l} - (c_w - c_o)}$$

and the limit a_o is

$$a_o = m_l \frac{x+\beta y+(c_w-c_o)}{x+\beta y-m_l(c_w-c_o)}$$

The superposition of the constant-lift sectors along the leading edge causes a decrement in pressure along the trailing edge and the tip which is not taken into account by the previously discussed corrections for these regions. The flow field corresponding to these pressure decrements is nonconical in form and must be evaluated by superposing constant-lift sectors to cancel the lift for each superposed leading-edge sector. Fortunately, in most cases the pressure decrements are so small they may be neglected.

If the Mach cone from the trailing edge of the control surface sweeps over the leading edge of the wing, an additional computation using a revised form of equation (11) must be made. In this case, the lifting pressures to be added ahead of the wing leading edge are those necessary to cancel the negative pressures resulting from the trailing-edge corrections of equations (7) or (9).

For a single control surface, such as an aileron, the distribution of the basic lift along the trailing edge given by the function G may, for the purpose of obtaining the negative pressure field ahead of the wing, be replaced by a step distribution which is canceled along the trailing edge by oblique triangles of finite lift placed at the steps. Each of these canceling triangles has a conical pressure field which may be corrected for ahead of the wing by equation (11) if the term G' in this equation is replaced by the equivalent derivative for the pressure field of the triangle superposed at the step. In equation (11), a then refers to a ray from the apex of the triangle superposed at the tip. The limits of the integral and the expression for t_a must be revised accordingly.

For adjacent control surfaces of equal deflection such as the elevators of figure 1, the correction needed to eliminate the negative pressures ahead of the wing resulting from the trailing-edge correction may be simplified by retaining only the conical flow field due to the first term of equation (9). This flow field may be treated in the same manner as for the basic lift (equation (11)).

CONTROL-SURFACE PARAMETERS

It has been shown by the previous discussion that the pressure at any point on the wing may be determined for a variety of plan forms

with sufficient accuracy for estimating control-surface parameters. Unfortunately it is not possible to express the parameters in closed form for most cases. In general, the induced lift and hinge-moment must be evaluated graphically.

In order to maintain maximum accuracy in estimating the parameters C_{h_δ}, C_{L_δ}, C_{l_δ}, C_{m_δ}, etc., it is suggested that the following procedure be followed:

(a) Evaluate the parameters for the basic lift by integrating analytically the basic-pressure distributions over the zone of influence of the control surface.

(b) Determine the induced effects due to interaction around the subsonic edges of the plan form by plotting the induced pressures at various spanwise stations and integrating mechanically to obtain forces and moments.

Then for example,

$$C_{L_\delta} = \left(C_{L_\delta}\right)_{basic} + \Delta C_{L_\delta}{}_{TE} + \Delta C_{L_\delta}{}_{tip} + \Delta C_{L_\delta}{}_{LE}$$

Because of the great number of equations needed to cover all variations in control-surface span, wing aspect ratio and taper ratio for the control-surface parameters for the basic lift, no attempt has been made to develop them here. In the succeeding sections, expressions for some of the parameters for the basic lift have been developed in integral form to act as a guide for the reader in setting up expressions for any particular plan form. Only control surfaces that extend to the tip of the wing are treated.

Variation of the Basic Lift Coefficient with Control Deflection at Constant Angle of Attack, $\left(C_{L_\delta}\right)_{basic}$

For a control surface of arbitrary plan form

$$\frac{\text{Lift}}{q} = \int \frac{\Delta p}{q}\, dA$$

where the integration must be carried out over the entire surface influenced by the control. For plan forms such as those of figure 1 with a tip cut off parallel to the direction of flight, the

integration must be carried out over the various regions where the elementary area dA between the ray a and the ray a+da retains the same form. In general, three regions must be dealt with, one between the Mach cone $a = -1$ and the ray passing through the trailing edge of the tip, a_t; the second between the ray a_t and the ray passing through the leading edge of the tip, a_l; and the third between the ray a_l and the Mach cone at $a=1$. It is found that

$$dA = \frac{m_t^2 c_o^2}{2\beta (m_t - a)^2} \, da \text{ from } a = -1 \text{ to } a_t$$

$$dA = \frac{\beta^2 s^2}{2\beta a^2} \, da \text{ from } a = a_t \text{ to } a = a_l$$

$$dA = \frac{m_l^2 (c_w - c_o)^2}{2\beta (a - m_l)^2} \, da \text{ from } a_l \text{ to } a = +1$$

Then for a subsonic hinge line and tip alined with the stream

$$\left(\beta C_{L_\delta}\right)_{basic} = \frac{\beta L}{qS\delta} = \frac{4}{\pi\beta S} \frac{m^2}{\sqrt{(\beta^2+m^2)(1-m^2)}} \left[\int_{-1}^{a_t} \frac{m_t^2 c_o^2}{2(m_t - a)^2} G(a) \, da \right.$$

$$\left. + \int_{a_t}^{a_l} \frac{\beta^2 s^2}{2a^2} G(a) \, da + \int_{a_l}^{1} \frac{m_l^2 (c_w - c_o)^2}{2(a - m_l)^2} G(a) \, da \right] \qquad (12)$$

where

$$a_t = \frac{\beta s}{c_o + \frac{\beta s}{m_t}}$$

and

$$a_l = \frac{\beta s}{\frac{\beta s}{m_l} - (c_w - c_o)}$$

This expression may be evaluated by integrating by parts. It should be noted that the last integral disappears if the Mach cone of the control surface does not cross the leading edge of the wing and the upper limit of the second integral becomes 1.

For a supersonic hinge line and tip alined with the stream

$$\left(\beta C_{L_\delta}\right)_{basic} = \frac{4}{\pi\beta S}\frac{m^2}{\sqrt{(\beta^2+m^2)(m^2-1)}}\left[\int_{-1}^{a_t}\frac{m_t^2 c_o^2}{2(m_t-a)^2}F(a)\,da + \int_{a_t}^{1}\frac{\beta^2 s^2}{2a^2}F(a)\,da + \frac{\pi}{2}\frac{\beta^2 s^2}{m}(m-1)\right] \quad (13)$$

If the tip is cut off perpendicular to the direction of flight, the area term in the second integral of these equations becomes $\frac{1}{2}\left[\frac{\beta s}{m_l} - (c_w - c_o)\right]^2 da$ instead of $\frac{\beta^2 s^2}{2a^2} da$, and the last term in equation (13) becomes $\frac{\pi}{2}(m-1)\left[\frac{\beta s}{m_l} - (c_w - c_o)\right]^2$

If the control surfaces considered are adjacent elevators, then the lower limit of the first integral of equations (12) and (13) becomes zero.

Variation of the Basic Rolling-Moment Coefficient with Control-Surface Deflection at Constant Angle of Sideslip, $\left(C_{l_\delta}\right)_{basic}$

The rolling moment produced by unit opposite deflection of partial-span ailerons, which do not have overlapping zones of influence, is

$$\frac{L}{q} = 2\int\frac{\Delta p}{q}(b_1+l_1)\,dA$$

where b_1 is the distance from the center line to the inboard end of the aileron and l_1 is the distance from the inboard end of the aileron to the center of pressure of the lift over area dA.

$$l_1 = \frac{2}{3}\frac{am_t}{\beta(m_t-a)}c_o \text{ from } a = -1 \text{ to } a = a_t$$

$$= \frac{2}{3}s \text{ from } a = a_t \text{ to } a = a_l$$

$$= \frac{2}{3}\frac{am_l(c_w-c_o)}{\beta(a-m_l)} \text{ from } a = a_l \text{ to } a = 1$$

For a subsonic hinge line and tip alined with the stream

$$\left(\beta C_{l_\delta}\right)_{basic} = \frac{\beta L}{qS\delta} = \frac{8}{\pi\beta S}\frac{m^2}{\sqrt{(\beta^2+m^2)(1-m^2)}}\left\{\int_{-1}^{a_t}\frac{m_t^2c_o^2}{2(m_t-a)^2}\left[\frac{b_1}{b}+\frac{2}{3}\frac{am_t}{(m_t-a)}\frac{c_o}{\beta b}\right]G(a)\,da\right.$$

$$\left.+\int_{a_t}^{a_l}\frac{\beta^2s^2}{2a^2}\left(\frac{b_1}{b}+\frac{2}{3}\frac{s}{b}\right)G(a)\,da+\int_{a_l}^{1}\frac{m_l^2(c_w-c_o)^2}{2(a-m_l)^2}\left[\frac{b_1}{b}+\frac{2}{3}\frac{am_l}{a-m_l}\frac{(c_w-c_o)}{\beta b}\right]G(a)\,da\right\} \quad (14)$$

For a supersonic hinge line

$$\left(\beta C_{l_\delta}\right)_{basic} = \frac{8}{\pi\beta S}\frac{m^2}{\sqrt{(\beta^2+m^2)(m^2-1)}}\left\{\int_{-1}^{a_t}\frac{m_t^2c_o^2}{2(m_t-a)^2}\left[\frac{b_1}{b}+\frac{2}{3}\frac{am_t}{(m_t-a)}\frac{c_o}{\beta b}\right]F(a)\,da\right.$$

$$\left.+\int_{a_t}^{1}\frac{\beta^2s^2}{2a^2}\left(\frac{b_1}{b}+\frac{2}{3}\frac{s}{b}\right)F(a)\,da+\frac{\pi}{2}\frac{(m-1)}{m}\beta^2s^2\left(\frac{b_1}{b}+\frac{2}{3}\frac{s}{b}\right)\right\} \quad (15)$$

If the tip is cut off perpendicular to the line of flight, the second integral in both these equations is changed to have the area term mentioned previously and a lever arm term of

$$\left\{ \frac{b_1}{b} + \frac{2}{3} \frac{a}{\beta b} \left[\frac{\beta s}{m_l} - (c_w - c_o) \right] \right\}$$

and becomes

$$\int \frac{l}{2} \left[\frac{\beta s}{m_l} - (c_w - c_o) \right] \left\{ \frac{b_1}{b} + \frac{2}{3} \frac{a}{\beta b} \left[\frac{\beta s}{m_l} - (c_w - c_o) \right] \right\} G(a) \text{ or } F(a)\, da$$

the last term of equation (15) becomes

$$\frac{\pi}{2} (m-1) \left[\frac{\beta s}{m_l} - (c_w - c_o) \right]^2 \left\{ \frac{b_1}{b} + \frac{m+1}{3} \left[\frac{\beta s}{m} - (c_w - c_o) \right] \right\}$$

Variation of the Basic Hinge-Moment Coefficient with Control-Surface Deflection, $\left(C_{h_\delta}\right)_{basic}$

The hinge moment of a control surface similar to an aileron with no overlapping zones of influence is given as

$$\frac{H}{q} = \int \frac{\Delta p}{q} l_2 \, dA$$

where l_2 is the lever arm of the lift over area dA about the hinge line. When the tip is alined with the stream

$$l_2 = \frac{2}{3} \frac{m}{\sqrt{\beta^2 + m^2}} \frac{m_t c_o}{(m_t - a)} \left(1 - \frac{a}{m}\right) \text{ between } a=0 \text{ and } a=a_t$$

$$l_2 = \frac{2}{3} \frac{m}{\sqrt{\beta^2 + m^2}} \frac{\beta s}{a} \left(1 - \frac{a}{m}\right) \text{ between } a=a_t \text{ and } a=m$$

For a subsonic hinge line

$$\left(\beta C_{h_\delta}\right)_{basic} = \frac{\beta M}{q b \bar{c}^2} = \frac{4}{\beta \pi b \bar{c}^2} \frac{m^2}{\sqrt{(\beta^2+m^2)(1-m^2)}} \left[\int_0^{a_t} \frac{m}{3\sqrt{1+m^2}} \frac{m_t^3 c_o^3}{(m_t-a)^3} \left(1 - \frac{a}{m}\right) G(a)\, da \right.$$

$$\left. + \int_{a_t}^{m} \frac{m}{\sqrt{1+m^2}} \frac{\beta^3 s^3}{3a^3} \left(1 - \frac{a}{m}\right) G(a)\, da \right] \tag{16}$$

For a supersonic hinge line

$$\left(\beta C_{h_\delta}\right)_{basic} = \frac{4}{\pi \beta b \bar{c}^2} \frac{m^2}{\sqrt{(\beta^2+m^2)(m^2-1)}} \left[\int_0^{a_t} \frac{m}{3\sqrt{\beta^2+m^2}} \frac{m_t^3 c_o^3}{(m_t-a)^3} \left(1 - \frac{a}{m}\right) F(a)\, da \right.$$

$$\left. + \int_{a_t}^{1} \frac{m}{\sqrt{1+m^2}} \frac{\beta^3 s^3}{3a^3} \left(1 - \frac{a}{m}\right) F(a)\, da + \frac{\pi}{6} \frac{(m-1)^2}{\sqrt{1+m^2}} \frac{\beta^3 s^3}{m} \right] \tag{17}$$

If the tip is cut off perpendicular to the line of flight, the second integrals of equations (16) and (17) become

$$\int \frac{m}{3\sqrt{\beta^2+m^2}} \left[\frac{\beta s}{m_l} - (c_w - c_o) \right]^3 \left(1 - \frac{a}{m}\right) G(a)\, da$$

or

$$\int \frac{m}{3\sqrt{\beta^2+m^2}} \left[\frac{\beta s}{m_l} - (c_w - c_o) \right]^3 \left(1 - \frac{a}{m}\right) F(a)\, da$$

with proper limits substituted and the last term of equation (17) becomes

$$\frac{\pi}{6} \frac{(m-1)^2}{\sqrt{\beta^2+m^2}} \left[\frac{\beta s}{m_l} - (c_w - c_o) \right]^3$$

Variation of the Basic Pitching-Moment Coefficient with Control-Surface Deflection at Constant Angle of Attack, $\left(C_{m_\delta}\right)_{basic}$

The pitching moment about an axis through the apex of the leading edge of the wing due to a control surface similar to the ailerons of figure 1(a) used for longitudinal control is

$$\frac{M}{q} = \int \frac{\Delta p}{q} (X+l_s)\, dA$$

where X is the distance in the x direction from the leading edge vertex to the vertex of the control surfaces and l_s the distance from the control-surface vertex to the center of pressure of the lift over area dA.

For both ailerons, if the hinge lines are subsonic and the tips are alined with the stream

$$\left(\beta C_{m_\delta}\right)_{basic} = \frac{\beta M}{qS\delta c_a} = \frac{8}{\pi\beta S} \frac{m^2}{\sqrt{(\beta^2+m^2)(1-m^2)}} \left[\int_{-1}^{a_t} \frac{m_t^2 c_o^2}{2(m_t-a)^2} \left(\frac{X}{c_a} + \frac{2}{3} \frac{m_t c_o}{(m_t-a)c_a} \right) G(a)\, da \right.$$

$$\left. + \int_{a_t}^{a_l} \frac{\beta^2 s^2}{2a^2} \left(\frac{X}{c_a} + \frac{2}{3} \frac{\beta s}{a c_a} \right) G(a)\, da + \int_{a_l}^{1} \frac{m_l^2 (c_w-c_o)^2}{2(a-m_l)^2} \left(\frac{X}{c_a} + \frac{2}{3} \frac{m_l}{(a-m_l)} \frac{(c_w-c_o)}{c_a} \right) G(a)\, da \right] \quad (18)$$

for the supersonic hinge line

$$\left(\beta C_{m_\delta}\right)_{basic} = \frac{8}{\pi\beta S} \frac{m^2}{\sqrt{(\beta^2+m^2)(m^2-1)}} \left\{ \int_{-1}^{a_t} \frac{m_t^2 c_o^2}{2(m_t-a)^2} \left(\frac{X}{c_a} + \frac{2}{3} \frac{m_t c_o}{(m_t-a)c_a} \right) F(a)\, da \right.$$

$$+ \int_{a_t}^{1} \frac{\beta^2 s^2}{2a^2} \left(\frac{X}{c_a} + \frac{2}{3} \frac{\beta s}{a c_a} \right) F(a)\, da$$

$$\left. + \frac{\pi}{2} \frac{\beta^2 s^2}{m} (m-1) \left[\frac{X}{c_a} + \frac{\beta s}{3m} \left(\frac{m+1}{c_a} \right) \right] \right\} \qquad (19)$$

For adjacent controls such as elevators the conjugate $\cosh^{-1}$ or $\cos^{-1}$ terms are added.

For a wing with the tip cut off perpendicular to the line of flight, the second integral of equations (18) and (19) becomes

$$\int \frac{1}{2} \left[\frac{\beta s}{m_l} - (c_w - c_o) \right]^2 \left\{ \frac{X}{c_a} + \frac{2}{3c_a} \left[\frac{\beta s}{m_l} - (c_w - c_o) \right] \right\} \left[G(a) \text{ or } F(a) \right] da$$

with appropriate limits.

The last term of equation (19) becomes

$$\frac{\pi(m-1)}{2} \left[\frac{\beta s}{m_l} - (c_w - c_o) \right]^2 \left\{ \frac{X}{c_a} + \frac{2}{3c_a} \left[\frac{\beta s}{m_l} - (c_w - c_o) \right] \right\}$$

Variation of Hinge-Moment Coefficient with Angle of Attack at Constant Control-Surface Deflection, C_{h_α}

Values of C_{h_α} may be calculated by the material of reference 2. It should be noted that values of C_{h_α} obtained for supersonic speeds are in general more negative than at subsonic speeds and therefore have a larger influence in determining the stick forces than at subsonic speeds.

ESTIMATED CHARACTERISTICS OF SPECIFIC CONTROL SURFACES

The distribution of lifting-pressure coefficients over several control surfaces has been calculated. The pressure distributions presented were determined by calculating the basic lifting pressures at various stations and correcting where necessary for the increments in pressure coefficient due to induction effects around the tip, trailing edge, and leading edge.

Elevators

Computations were made for the control surfaces of figure 4 for a Mach number of $\sqrt{2}$. Both control surfaces have areas equal to 20 percent of the total area. For the pressure distributions, the aspect ratio and taper ratio of the wings are significant only insofar as they affect the wing plan form within the zone of influence of the control surface. A solution for the control surfaces shown may be used for other aspect ratios and taper ratios if appropriate values of wing area and span are substituted in the expressions for the control-surface parameters. Figures 5(a) to (d) show the distribution of lifting-pressure coefficient along the chord at various spanwise stations. Section values of C_{L_δ} and C_{h_δ} are given at each station. The hinge-moment coefficients are based on the average chord in the stream direction for both the tapered and constant-chord control surfaces so that the values of C_{h_δ} are directly comparable.

The distribution of pressure along the root chord is seen to be similar to the Ackeret distribution. Proceeding toward the tip, the pressure distributions approach the familiar subsonic type of pressure distribution over flapped wings. The section hinge-moment coefficients for the constant-chord control surface are of the same order of magnitude as those experienced at subsonic speeds if they are multiplied by the ratio of free-stream dynamic pressure to the dynamic pressure based on the component of the free-stream velocity perpendicular to the leading edge.

Figures 6 and 7 show the spanwise variation of the section values of c_{L_δ} and c_{h_δ} and figure 8 shows the spanwise variation of c_{h_α} determined by the methods of reference 2. The curve of figure 8 shows the effect of the tip alined with the stream in reducing the lift within its Mach cone discussed in reference 2, thereby giving values of c_{h_α} near zero.

Integrated values of the control-surface parameters are as follows:

	Constant chord	Tapered chord
C_{L_δ}	0.392	0.338
C_{h_δ}	−.158	−.152
C_{L_α}	1.65	1.65
C_{h_α}	−.105	−.313
α_δ	−.238	−.205

(All values are for deflections and angles of attack in radians.)

The values of α_δ are of smaller magnitude than those for control surfaces of the same size at subsonic speeds. A comparison of the values of C_{h_δ} and C_{h_α} is of interest. It is evident that the value of C_{h_α} can be controlled nearly independently of C_{h_δ} and C_{L_δ} at any Mach number by varying the taper of the control surface. This is due first to the type of loading at the root and second to the large loss in the lift due to angle of attack which occurs within the Mach cone of the streamwise tip of a wing with subsonic leading edges. This variation in C_{h_α} with taper of the control surface is a function of aspect ratio (or of Mach number) becoming greater with lower aspect ratio (or lower Mach number).

Calculations for these two control surfaces with the tip cut off parallel to the stream were extended to the control surfaces of figure 9 which have the tip cut off perpendicular to the stream. Although this entails a change in aspect ratio, the results are still of interest. The chordwise pressure distributions for the first three spanwise stations in terms of the root chord of the control surface are the same as those of figures 5(a), (b), and (c). The pressure distributions over the three remaining spanwise stations are shown in figures 10(a), (b), and (c). The data of figure 10(c) show infinite pressure at the leading edge due to the upwash between the leading edge and the Mach cone.

Figures 11, 12, and 13 show the variation of section values of c_{L_δ}, c_{h_δ}, and c_{h_α} along the span, the constant-chord control surface having a span of 60 percent of the wing span and the tapered chord having a span of 50-percent wing span. Integrated values of the parameters are as follows:

	Constant chord	Tapered chord
C_{L_δ}	0.358	0.287
C_{h_δ}	−.172	−.155
C_{L_α}	3.03	3.03
C_{h_α}	−.193	−.348
α_δ	−.118	−.095

It should be noted that these control surfaces are not of the same area. The constant-chord control surface is 14.65 percent of the total area and the tapered chord is 13.33 percent of the total area.

The values of α_δ given in the table are much smaller than those for the control surfaces of figure 4 which have the tip alined with the stream, even considering the difference in the relative sizes of the control surfaces in terms of percentage of total area.

This is due to the fact that, as shown in reference 2, when the tip is alined with the stream most of the basic lift due to angle of attack is lost within the Mach cone from the leading edge of the tip; whereas when the tip is cut off perpendicular to the line of flight no lift is lost. Thus, for low aspect ratios and taper ratios near 1, the alinement of the tip has a powerful effect on C_{L_α}. A corresponding effect of tip alinement on C_{L_δ} occurs but is of much smaller magnitude than for C_{L_α}. The net result is that the ratio of C_{L_δ} to C_{L_α}, which is α_δ, is much greater for a given aspect ratio and control-surface size when the tip is alined with the stream than when it is cut off perpendicular to the direction of flight.

Aileron

The computations for the control surfaces of figure 4 were extended to a calculation of the characteristics of the ailerons of figure 14. Figure 15 shows the variation of pressure coefficients along the chord for the various spanwise stations. The spanwise variation of the section values of c_{L_δ} and c_{h_δ} are shown in

figure 16. The integrated values are given in the following table:

C_{L_δ} = 0.095 (one aileron)

C_{h_δ} = −.123

C_{l_δ} = 0.0711 (both ailerons)

C_{n_δ} = −0.0711α (both ailerons)

The significance of these values must await determination of the damping in roll and the rolling moment due to sideslip, which problems incidentally appear to be amenable to treatment by the methods of reference 2.

The remarks of the previous section relative to the effect of the alinement of the tip on α_δ for elevators apply in general to the ratio of C_{l_δ} to C_{l_p}. For low aspect ratios and taper ratios near 1, the effect of tip alinement on C_{l_p} will be very powerful; whereas the effect on C_{l_δ} will be small. It seems therefore that from the standpoint of obtaining large values of $pb/2V$ with small control surfaces, the tip of the wing should be alined with the stream.

Ames Aeronautical Laboratory,
National Advisory Committee for Aeronautics,
Moffett Field, Calif.

APPENDIX A

Evaluation of Integrals Expressing Superposition Process

The integral equation giving the induced lifting-pressure increments due to the interaction between the upper and lower surfaces of the wing around the streamwise tip for a control surface with a subsonic hinge line is

$$\Delta\left(\frac{\Delta p}{q}\right) = -\frac{\delta}{\beta}\frac{4}{\pi^2}\frac{m^2}{\sqrt{(\beta^2+m^2)(1-m^2)}}\int_1^{a_o} G'(a)\cos^{-1}\frac{a+t_a+2at_a}{t_a-a}\,da \qquad (A1)$$

with

$$t_a = \frac{\beta(y-s)}{x-\frac{\beta s}{a}}$$ and $G'(a)$ as discussed in the text.

This equation must be evaluated graphically. Unfortunately, the nature of the distribution of the basic lift due to the deflection of the control surface is such that $G'(a)$ is infinite at the Mach cone, $a=1$, and at the hinge line, $a=m$, changing sign as the hinge line is crossed.

If the integration of equation (A1) is carried to a value of a_o greater than m, the singularities at the hinge line, $a=m$, are not encountered. In this case, since the function $G(a)$ has the value of zero at $a=1$, equation (A1) may be rewritten in a form which may be evaluated graphically by replacing $G'(a)da$ by $dG(a)$.

$$\Delta\left(\frac{\Delta p}{q}\right)_{tip} = -\frac{\delta}{\beta}\frac{4}{\pi^2}\frac{m^2}{\sqrt{(\beta^2+m^2)(1-m^2)}}\int_0^{G(a_o)}\cos^{-1}\frac{a+t_a+2at_a}{t_a-a}\,dG(a) \tag{A2}$$

where $G(a_o)$ is the value of the function $G(a)$ at $a=a_o$.

If the integration of equation (A1) is carried to a value of a_o less than m, the function $G(a)$ as well as $G'(a)$ becomes infinite at $a=m$ and the method just discussed cannot be used. In this case, the integral may be rewritten as follows:

$$\int_1^{a_o} G'(a)\cos^{-1}\frac{a+t_a+2at_a}{t_a-a}\,da = \int_1^{m} G'(a)\cos^{-1}\frac{a+t_a+2at_a}{t_a-a}\,da + \int_m^{a_o} G'(a)\cos^{-1}\frac{a+t_a+2at_a}{t_a-a}\,da \tag{A3}$$

Considering the first integral of the right-hand side of equation (A3), the singularity at $a=1$ may be removed as follows:

$$\int_1^{m} G'(a)\cos^{-1}\frac{a+t_a+2at_a}{t_a-a}\,da = \int_1^{m} G'(a)\left(\cos^{-1}\frac{a+t_a+2at_a}{t_a-a} - K\right)da + K\int_1^{m} G'(a)\,da$$

when K is the value of $\cos^{-1}\frac{a+t_a+2at_a}{t_a-a}$ when $a=1$.

$$K = \cos^{-1}\frac{1+3t_1}{t_1-1}$$

when $a=1$, $G'(a)\left(\cos^{-1}\frac{a+t_a+2at_a}{t_a-a} - K\right)$ is indeterminate and may be evaluated as

$$\lim_{a\to 1} G'(a)\left(\cos^{-1}\frac{a+t_a+2at_a}{t_a-a} - K\right) = 0$$

since the derivative of the denominator is infinite at $a=1$, while that of the numerator is finite. $G'(a)\left(\cos^{-1}\frac{a+t_a+2at_a}{t_a-a} - K\right)$ may then be plotted from $a=1$.

To remove the singularities at both $a=1$ and $a=m$, the first integral of the right-hand side of equation (A3) may be rewritten as follows:

$$\int_1^m G'(a)\cos^{-1}\frac{a+t_a+2at_a}{t_a-a}\,da = \int_1^a G'(a)\left(\cos^{-1}\frac{a+t_a+2at_a}{t_a-a} - K\right)da + K\int_1^a G'(a)\,da$$

$$+\int_a^m G'(a)\left(\cos^{-1}\frac{a+t_a+2at_a}{t_a-a} - L\right)da + L\int_a^m G'(a)\,da \qquad (A4)$$

where L is the value of $\cos^{-1}\frac{a+t_a+2at_a}{t_a-a}$ at $a=m$

$$L = \cos^{-1}\frac{m+t_m+2mt_m}{t_m-m}$$

When $a=m$, $G'(a)\left(\cos^{-1}\frac{a+t_a+2at_a}{t_a-a}-L\right)$ is indeterminate.

By differentiating numerator and denominator once, it is found that

$$\lim_{a\to m} G'(a)\left(\cos^{-1}\frac{a+t_a+2at_a}{t_a-a}-L\right) = +\frac{1}{(t_m-m)\sqrt{-\frac{t_m(1+t_m)}{m(1+m)}}}\left[\frac{t_m(1+t_m)}{m(1+m)}-\frac{\beta(y-s)-xt_m}{mx-\beta s}\right]$$

and $G'(a)\left(\cos^{-1}\frac{a+t_a+2at_a}{t_a-a}-L\right)$ may be plotted to this value at $a=m$.

The second integral of the right-hand side of equation (A3) may be treated in the same manner.

$$\int_m^{a_o} G'(a)\cos^{-1}\frac{a+t_a+2at_a}{t_a-a} = \int_m^{a_o} G'(a)\left(\cos^{-1}\frac{a+t_a+2at_a}{t_a-a}-L\right)da + L\int_m^{a_o} G'(a)\,da \qquad (A5)$$

where L has the same value as for the previous case, since the singularity at $a=m$ is again to be removed.

The evaluation of the indeterminate quantity $G'(a)\left(\cos^{-1}\frac{a+t_a+2at_a}{t_a-a}-L\right)$ at $a=m$ gives the same value as for the previous case, but the sign is opposite because the lower limit is involved.

Equations (A4) and (A5) may now be combined to give

$$\int_1^{a_o} G'(a) \cos^{-1}\frac{a+t_a+2at_a}{t_a-a}\,da = \int_1^{a} G'(a)\left(\cos^{-1}\frac{a+t_a+2at_a}{t_a-a} - K\right)da + K\int_1^{a} G'(a)\,da$$

$$+ \int_a^{m} G'(a)\left(\cos^{-1}\frac{a+t_a+2at_a}{t_a-a} - L\right)da + L\int_a^{m} G'(a)\,da$$

$$+ \int_m^{a_o} G'(a)\left(\cos^{-1}\frac{a+t_a+2at_a}{t_a-a} - L\right)da + L\int_m^{a_o} G'(a)\,da$$

or

$$\int_1^{a_o} G'(a) \cos^{-1}\frac{a+t_a+2at_a}{t_a-a} = \int_1^{a} G'(a)\left(\cos^{-1}\frac{a+t_a+2at_a}{t_a-a} - K\right)da$$

$$+ \int_a^{a_o} G'(a)\left(\cos^{-1}\frac{a+t_a+2at_a}{t_a-a} - L\right)da + (K-L)\,G(a) + L\,G(a_o) \qquad (A6)$$

where $G(a_o)$ is the function $G(a)$ at $a=a_o$ and the limit a is any arbitrary value of a between $a=1$ and $a=m$.

The first and second integrals of equation (A6) may be evaluated graphically. (The second integral is plotted to the limiting value at $a=m$.)

The methods used above for the integration along the tip of a wing for a control surface with a subsonic hinge line may also be used along the trailing edge or leading edge to remove the singularities at the Mach cone $a = -1$ or $a = 1$ or at the hinge line $a = m$ for control surfaces,

the hinge lines of which intersect the leading or trailing edges.

The method of equation (A2) may be used for the singularity at the Mach cone for supersonic hinge lines.

REFERENCES

1. Jones, Robert T.: Thin Oblique Airfoils at Supersonic Speed. NACA TN No. 1107, 1946.

2. Cohen, Doris: The Theoretical Lift of Flat Swept-Back Wings at Supersonic Speeds. NACA TN No. 1555, 1948.

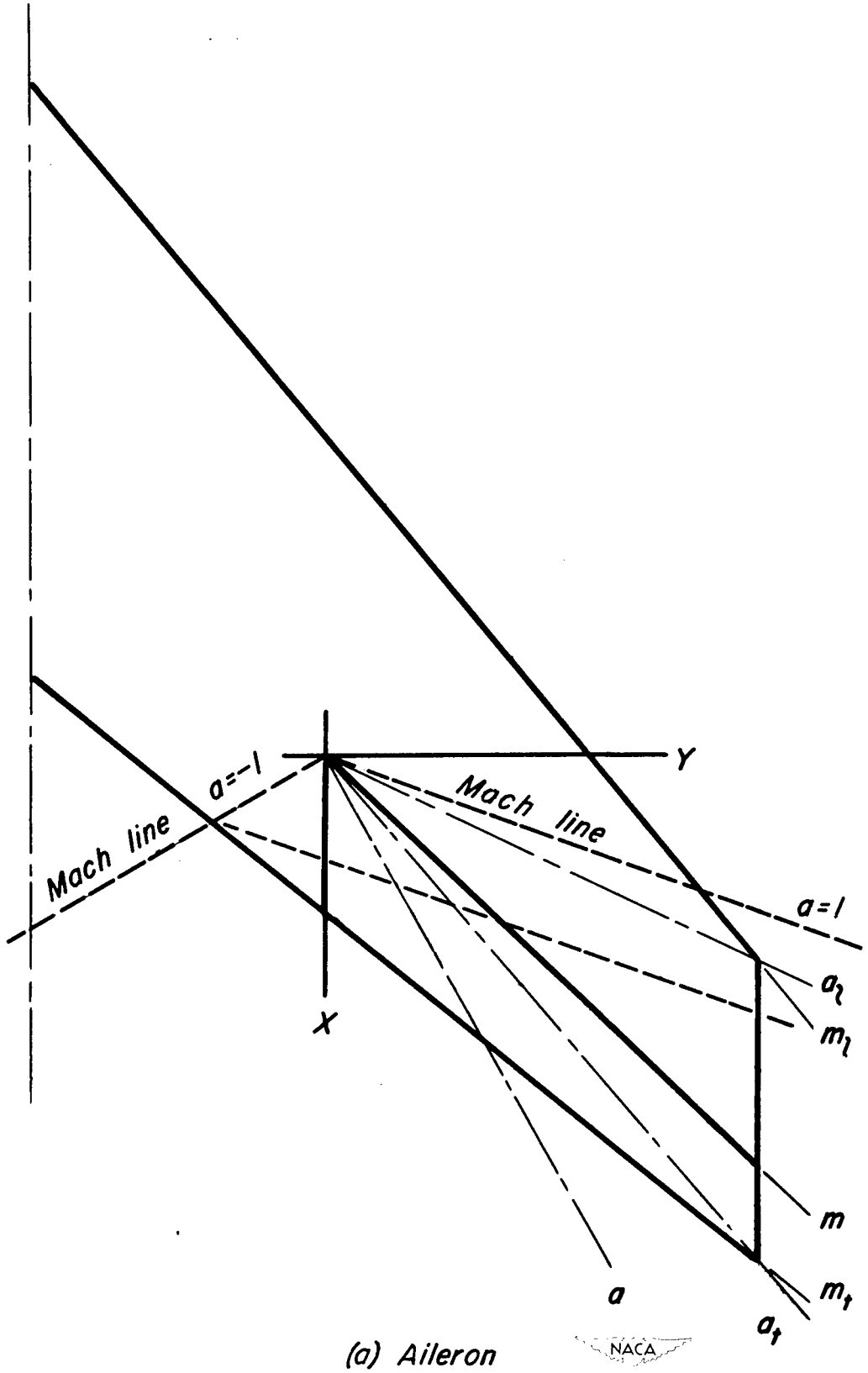

(a) Aileron

Figure 1.–Coordinate system for control suface calculations

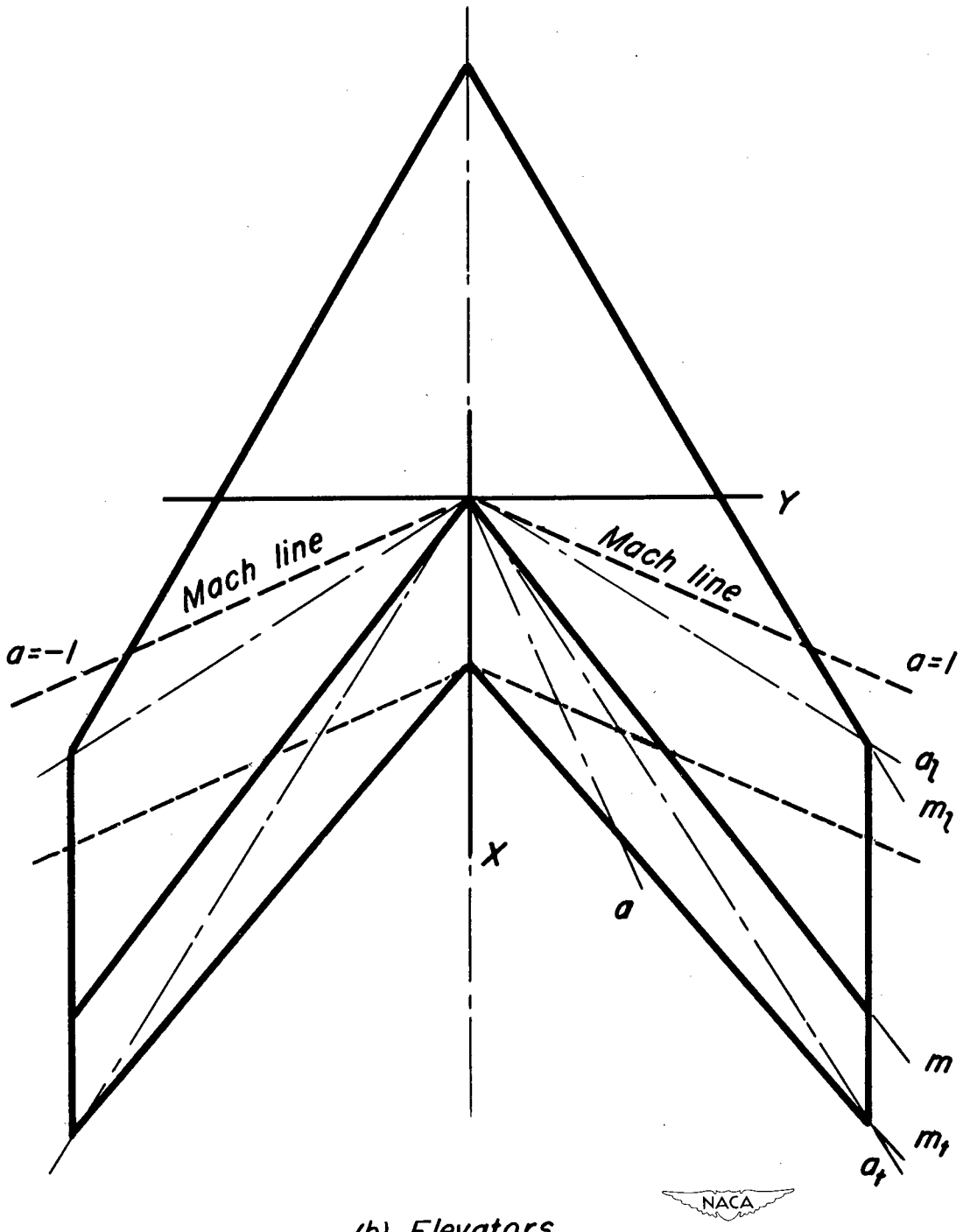

(b) Elevators

Figure 1.—Concluded

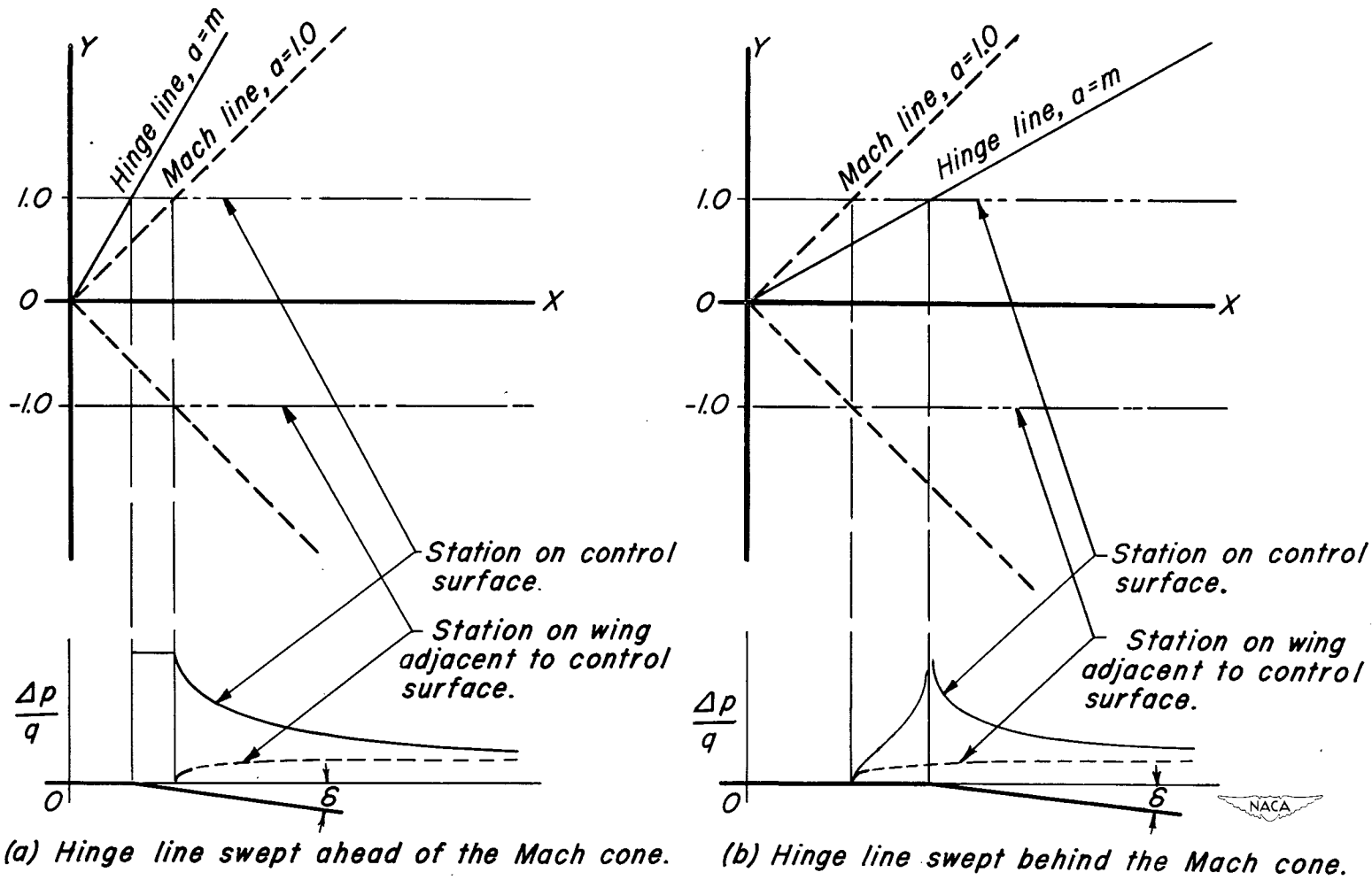

Figure 2.- Basic lifting-pressure distribution for control surfaces.

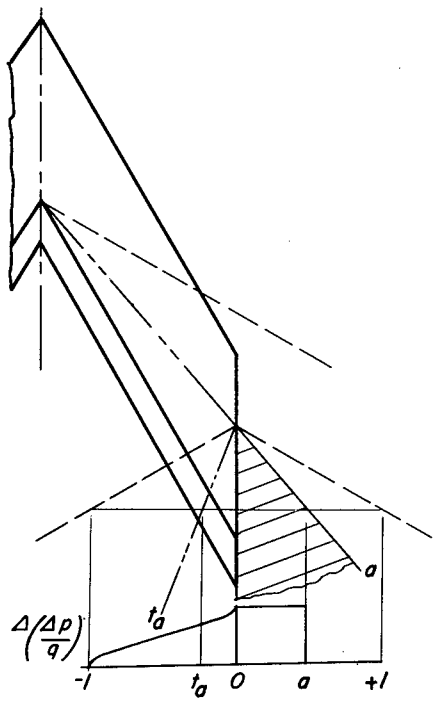

(a) Tip sector

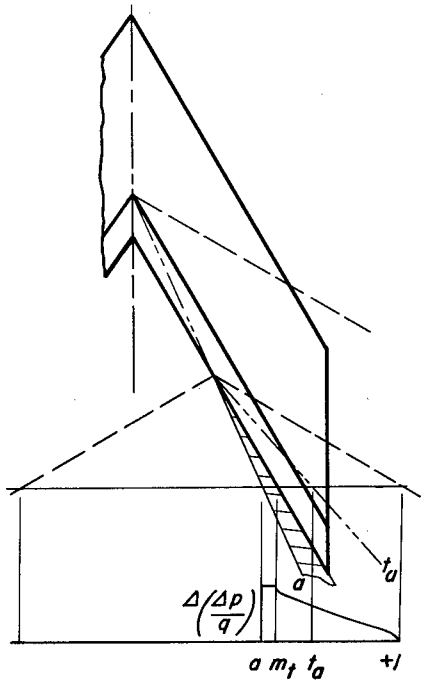

(b) Trailing edge oblique sector

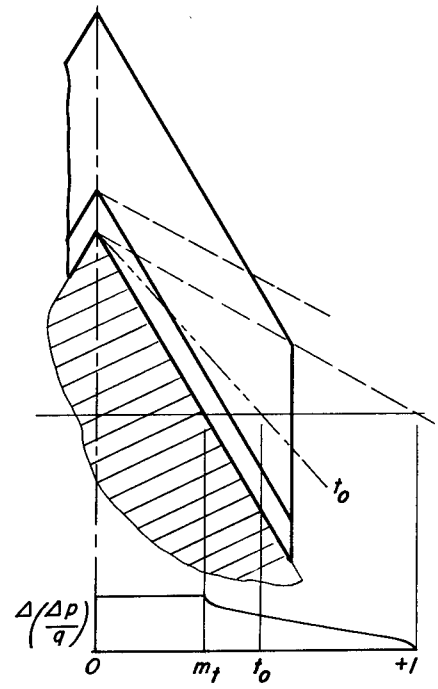

(c) Trailing edge symmetrical sector

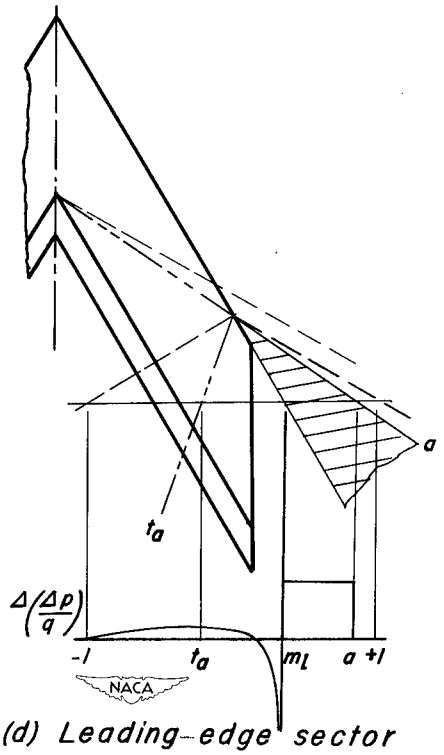

(d) Leading-edge sector

Figure 3.– Constant-load sectors used for superposition.

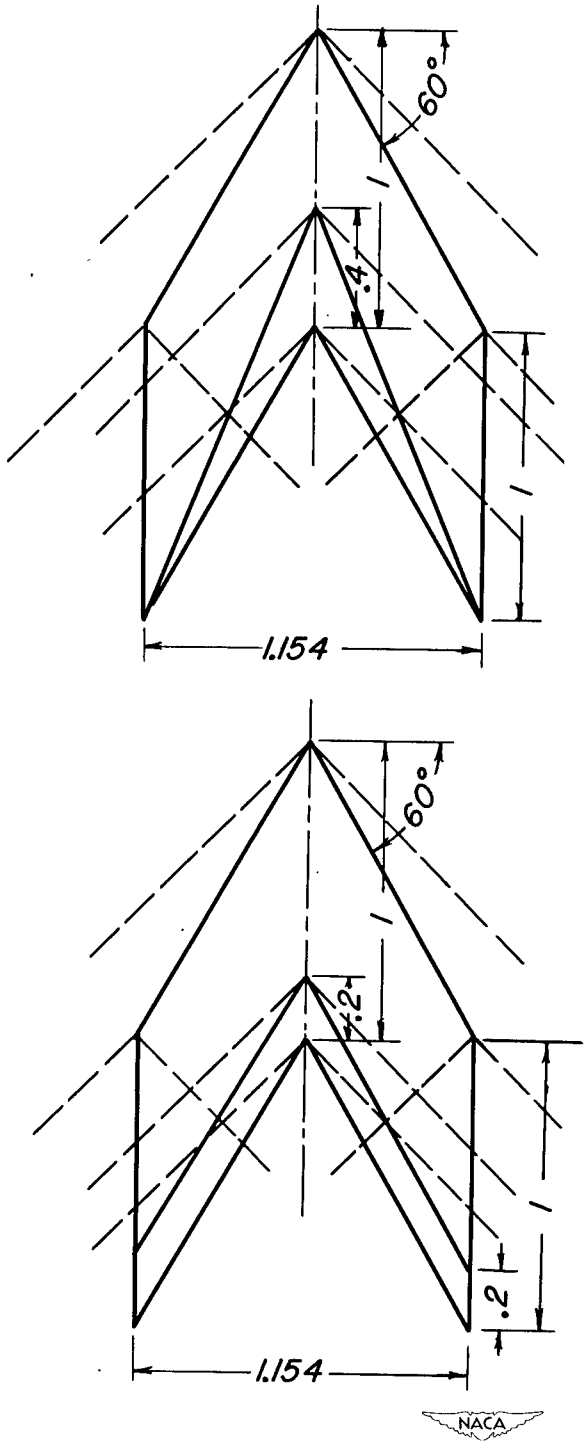

Figure 4.- Swept-back control surfaces with streamwise tips.

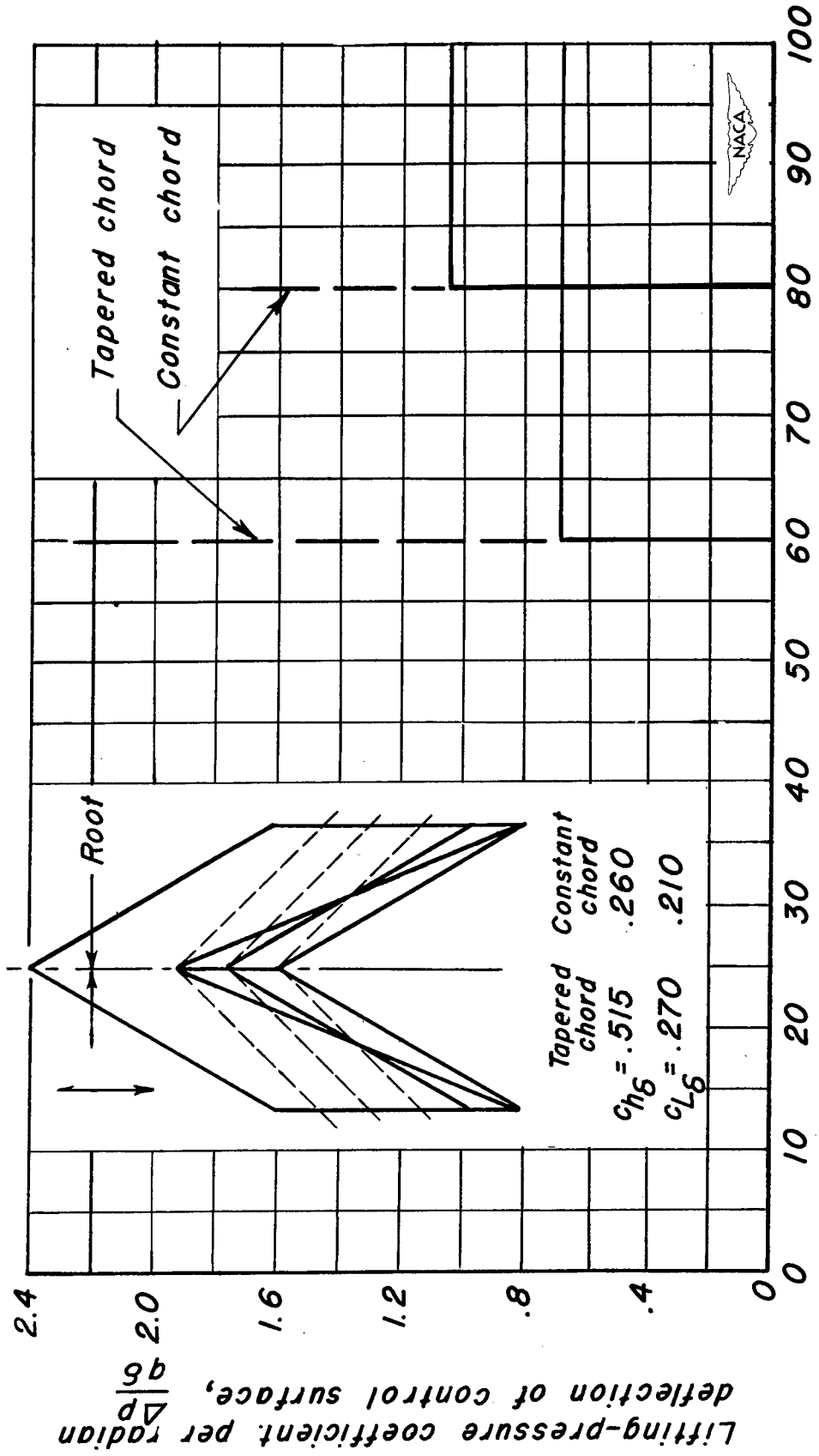

(a) Root

Figure 5.- Chordwise distribution of lifting-pressure coefficient for tapered and constant-chord control surfaces with streamwise tips.

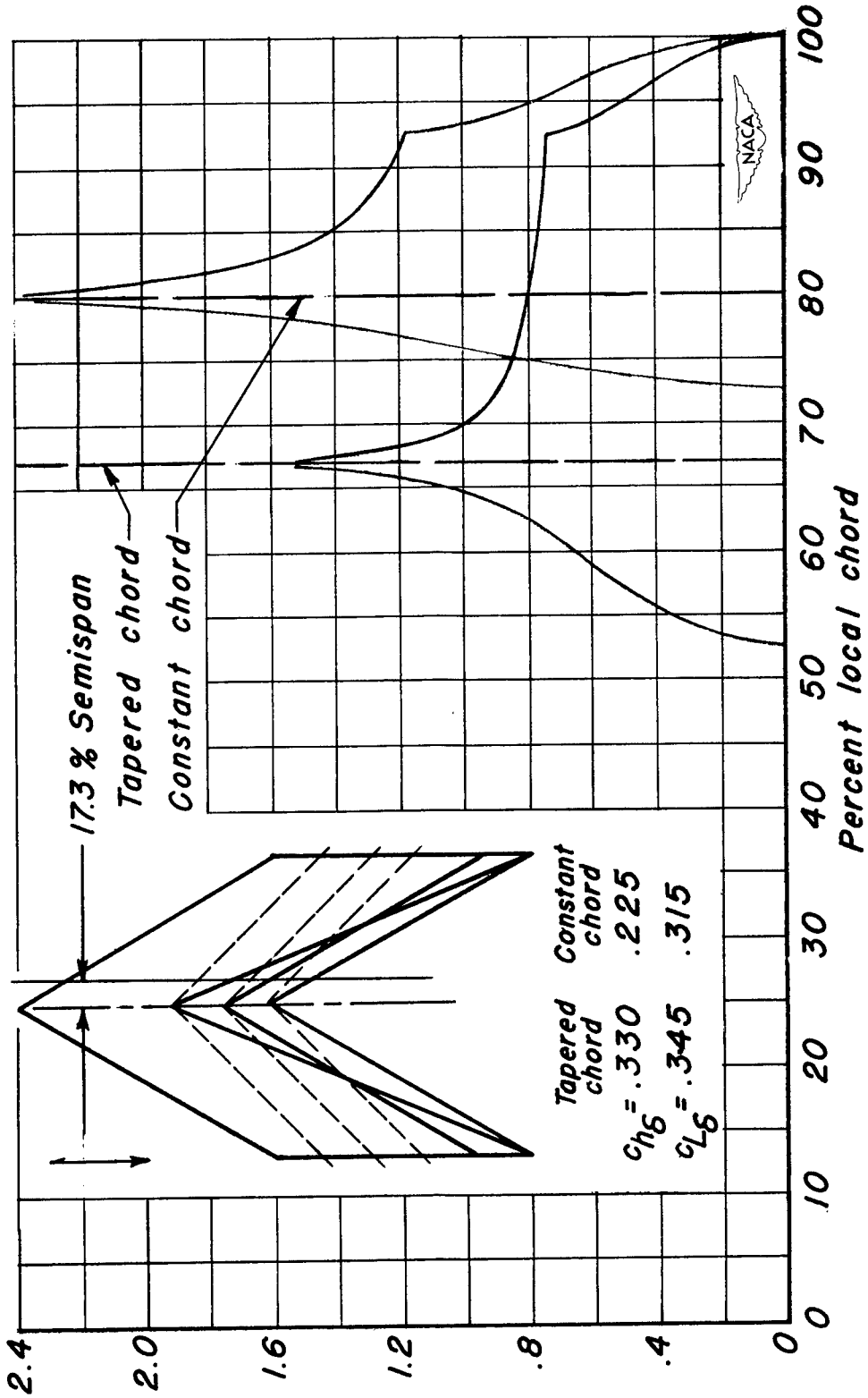

(b) 17.3 % Semispan

Figure 5.- Continued

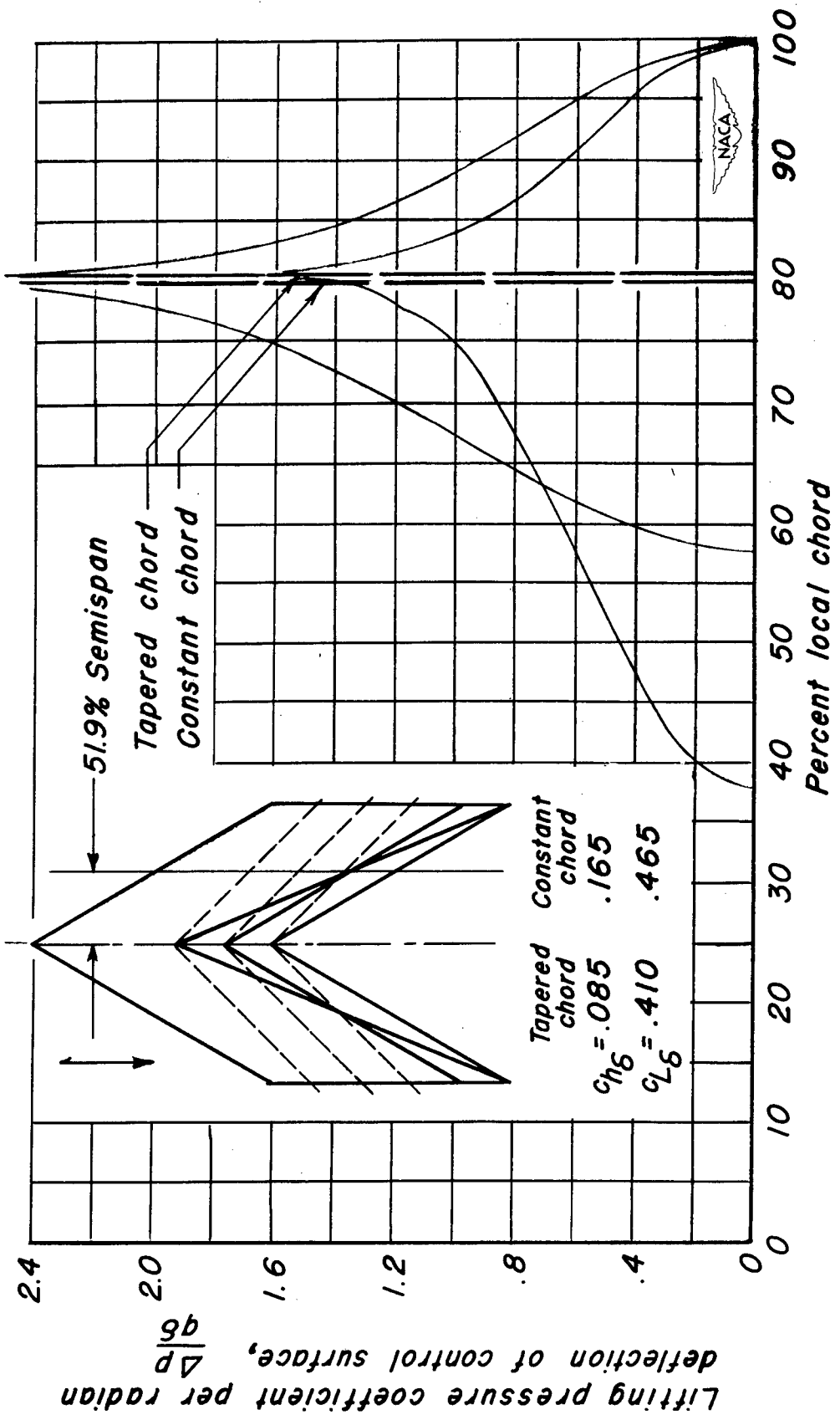

(c) 51.9 % Semispan

Figure 5.—Continued

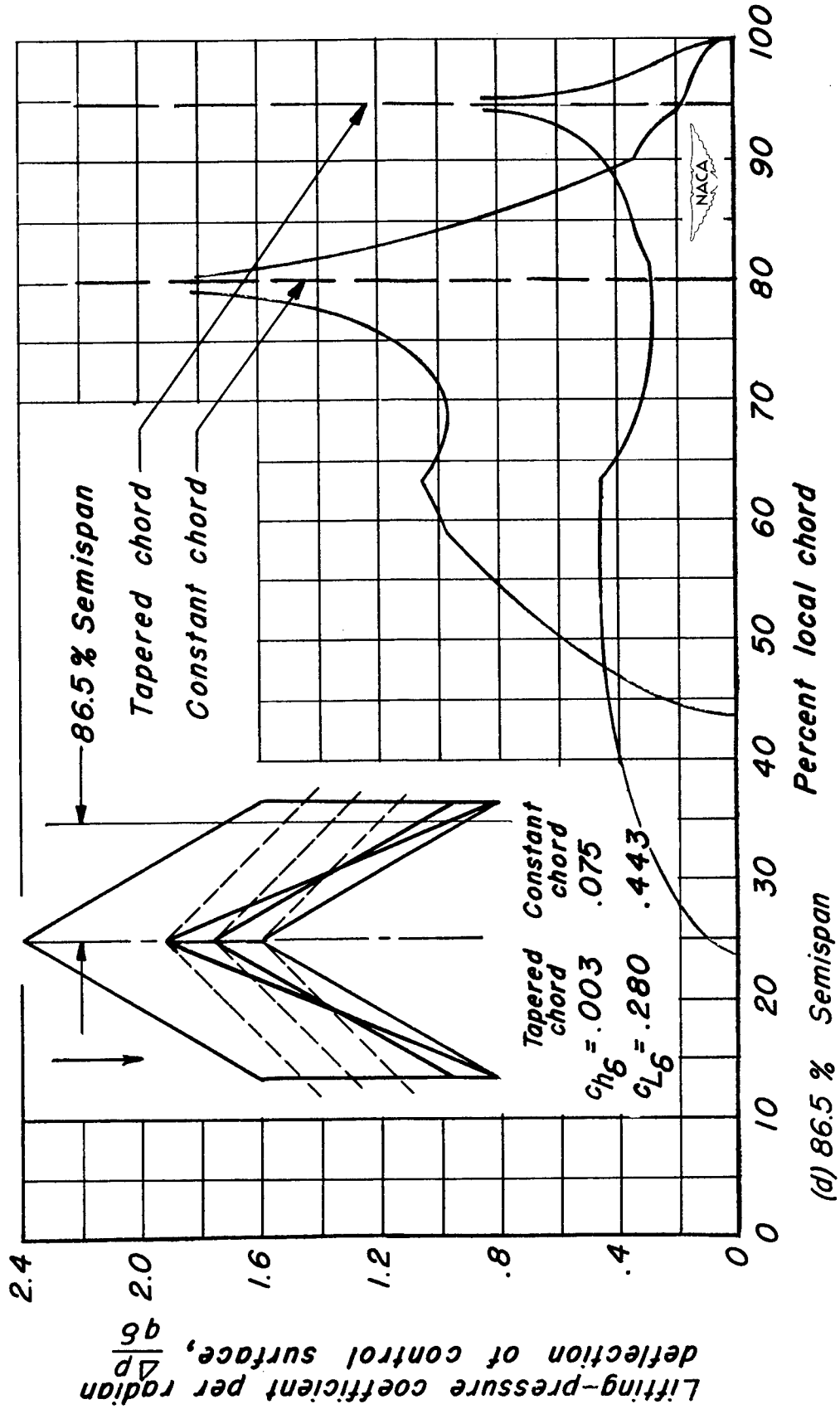

(d) 86.5 % Semispan

Figure 5.- Concluded

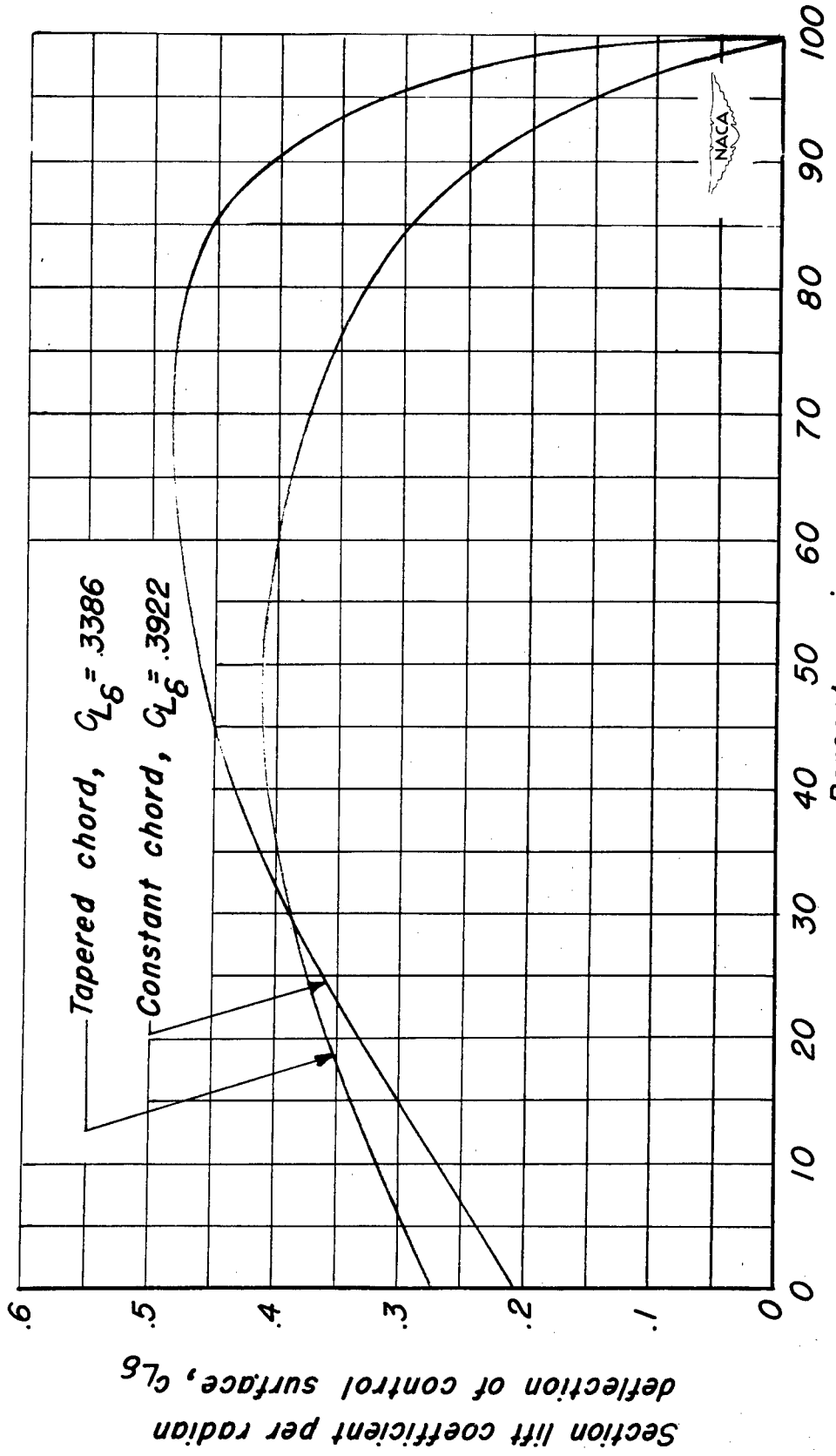

Figure 6.- Spanwise variation of the section values of c_{l_δ} for tapered and constant-chord control surfaces with streamwise tips.

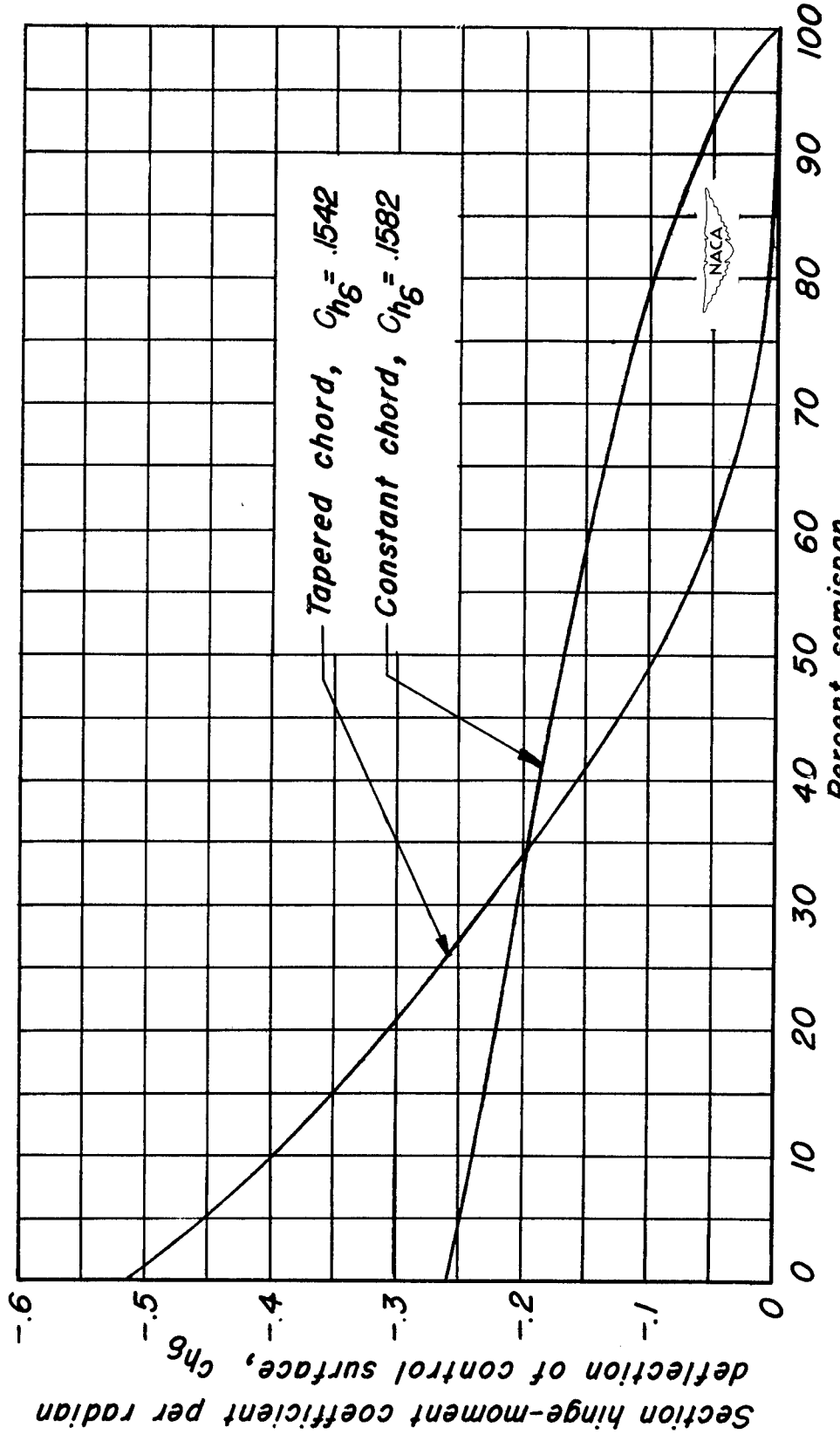

Figure 7.- Spanwise variation of the section values of c_{h_δ} for tapered and constant-chord control surfaces with streamwise tips.

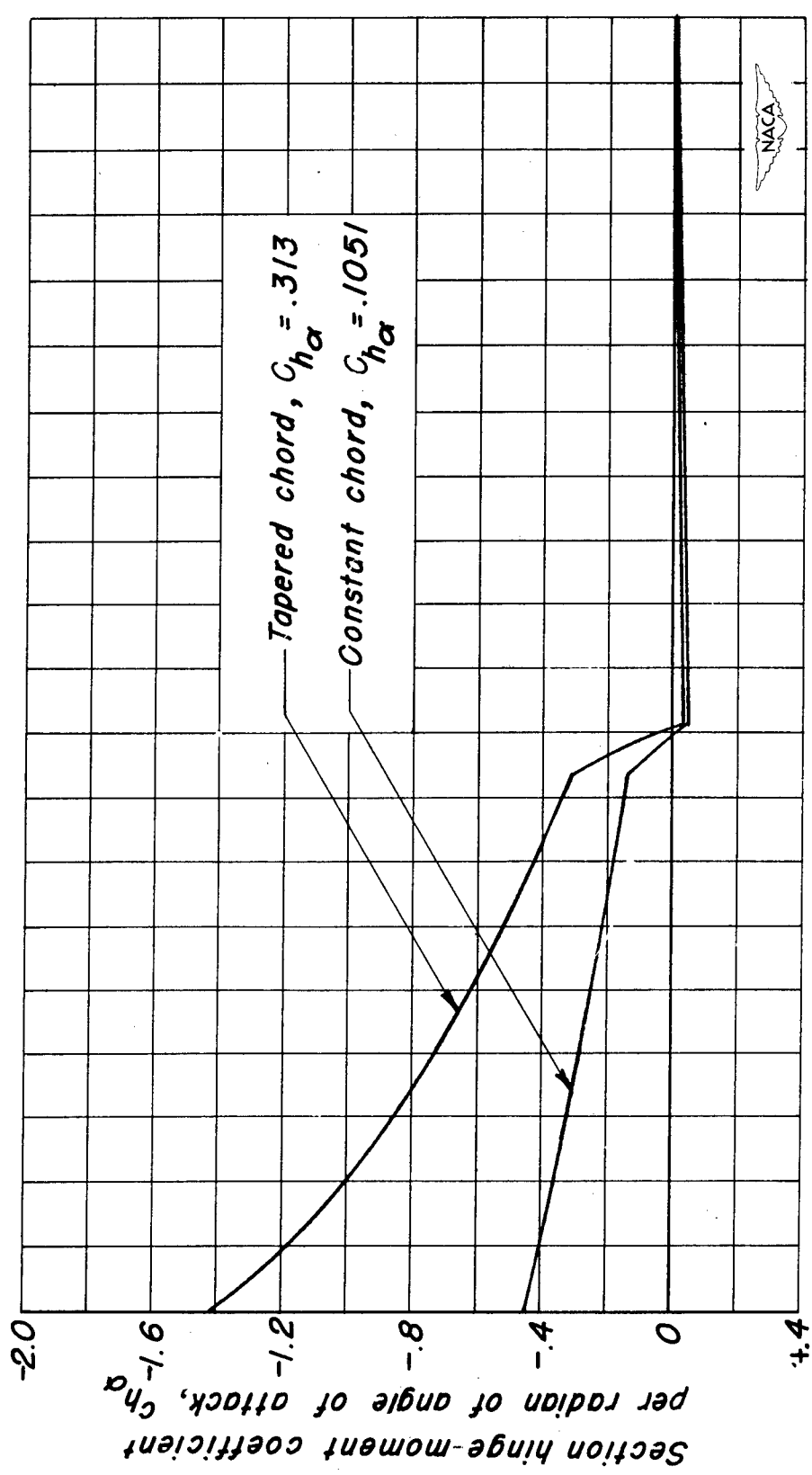

Figure 8.- Spanwise variation of the section values of c_{h_α} for tapered and constant-chord control surfaces with streamwise tips.

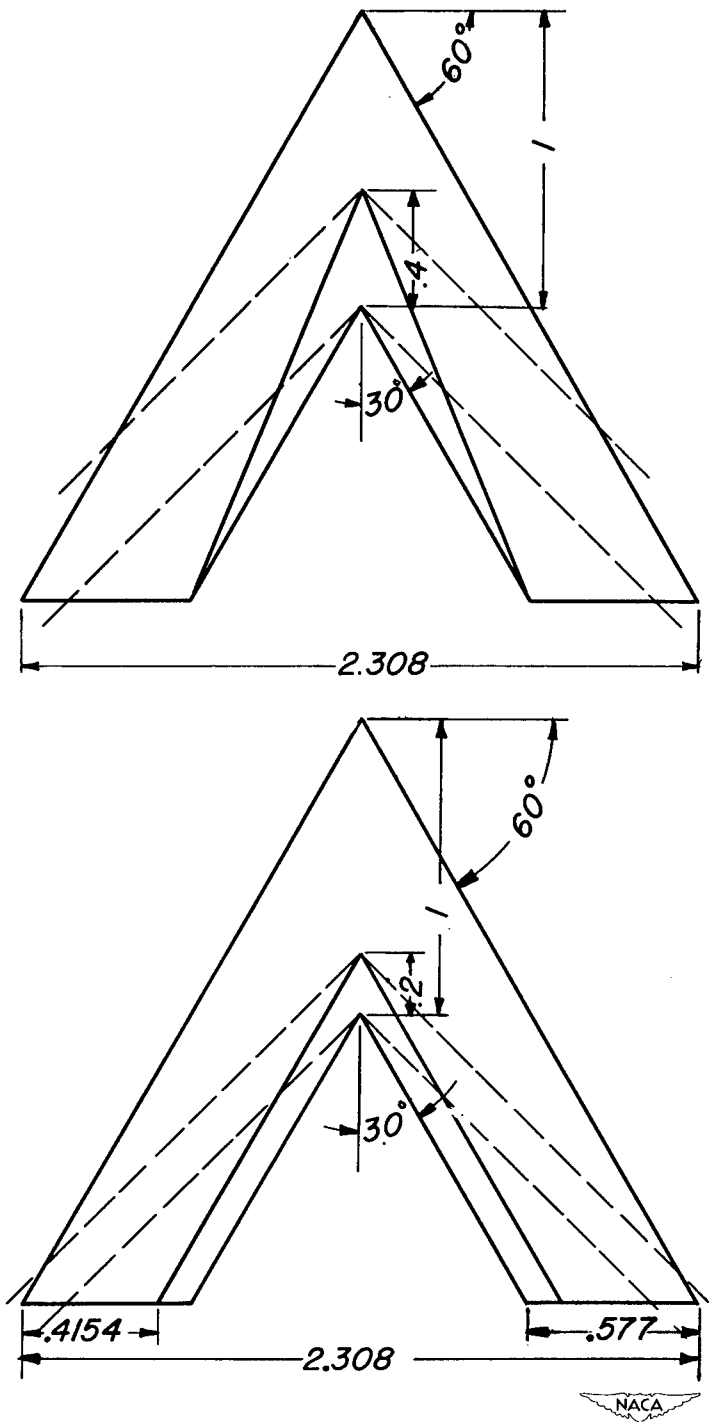

Figure 9.— Swept-back control surfaces with cross-stream tips.

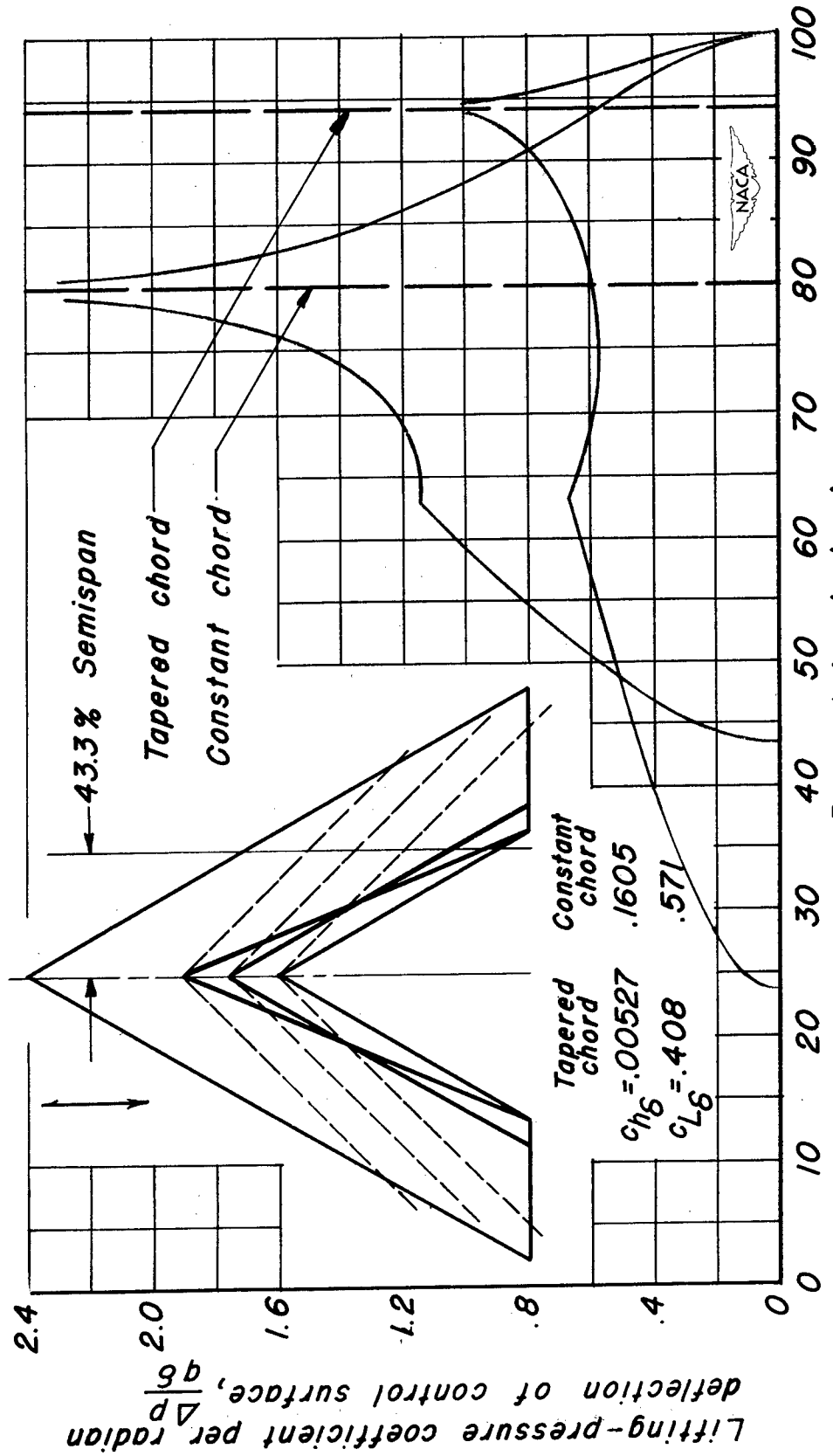

(a) 43.3 % Semispan

Figure 10.- Chordwise distribution of lifting-pressure coefficient for tapered and constant-chord control surfaces with cross-stream tips.

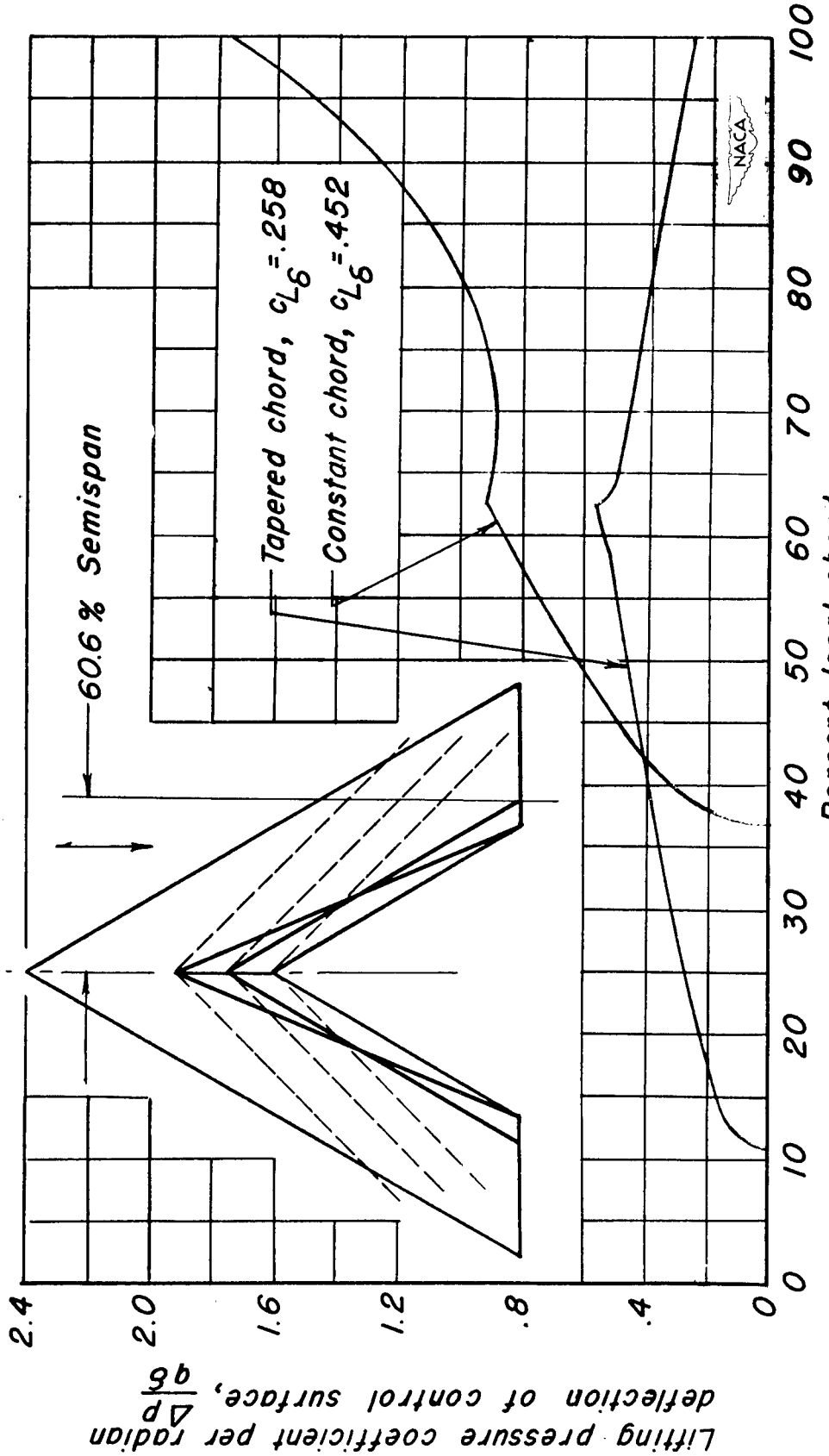

(b) 60.6 % Semispan

Figure 10.- Continued

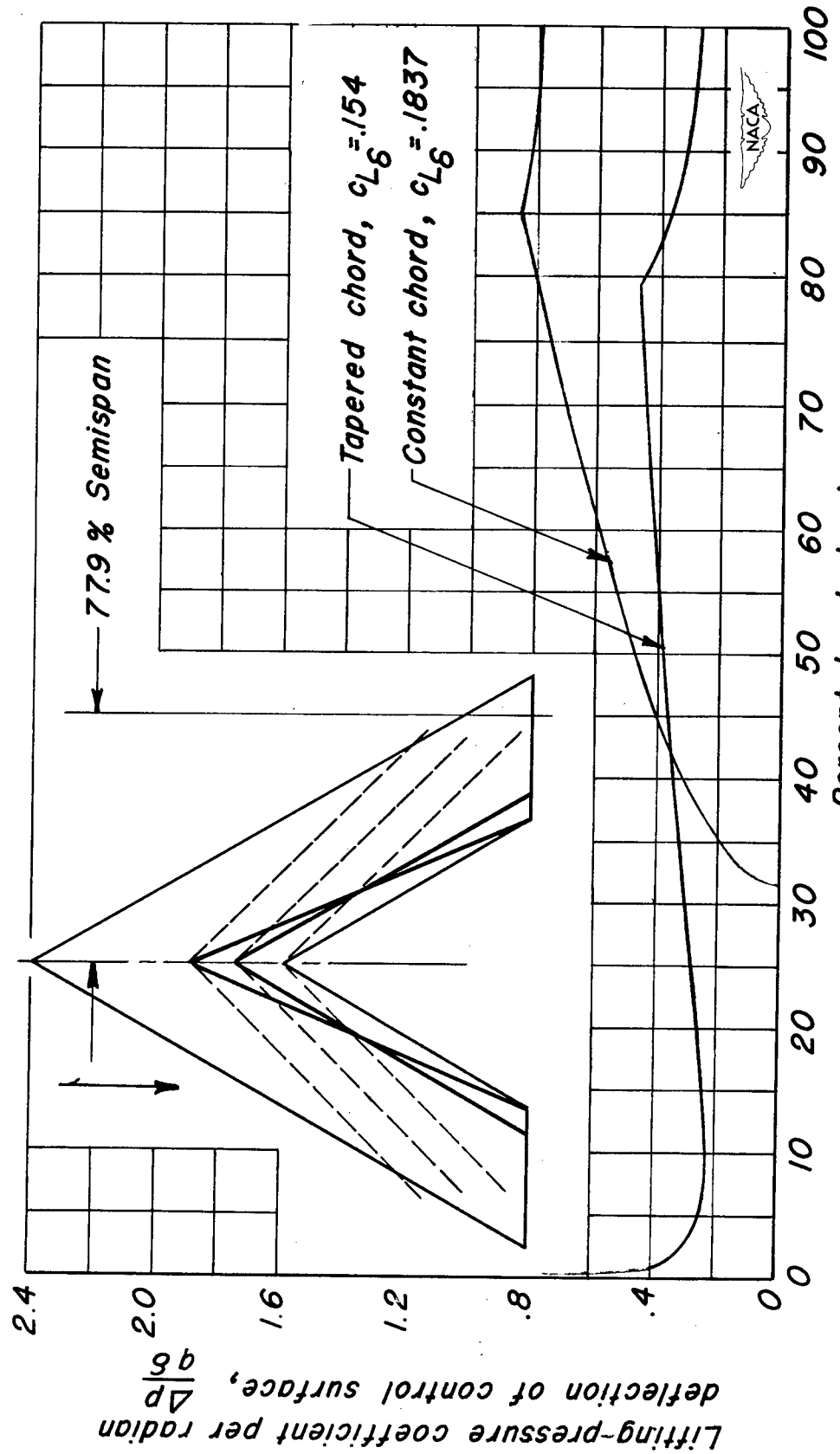

(c) 77.9 % Semispan

Figure 10.- Concluded

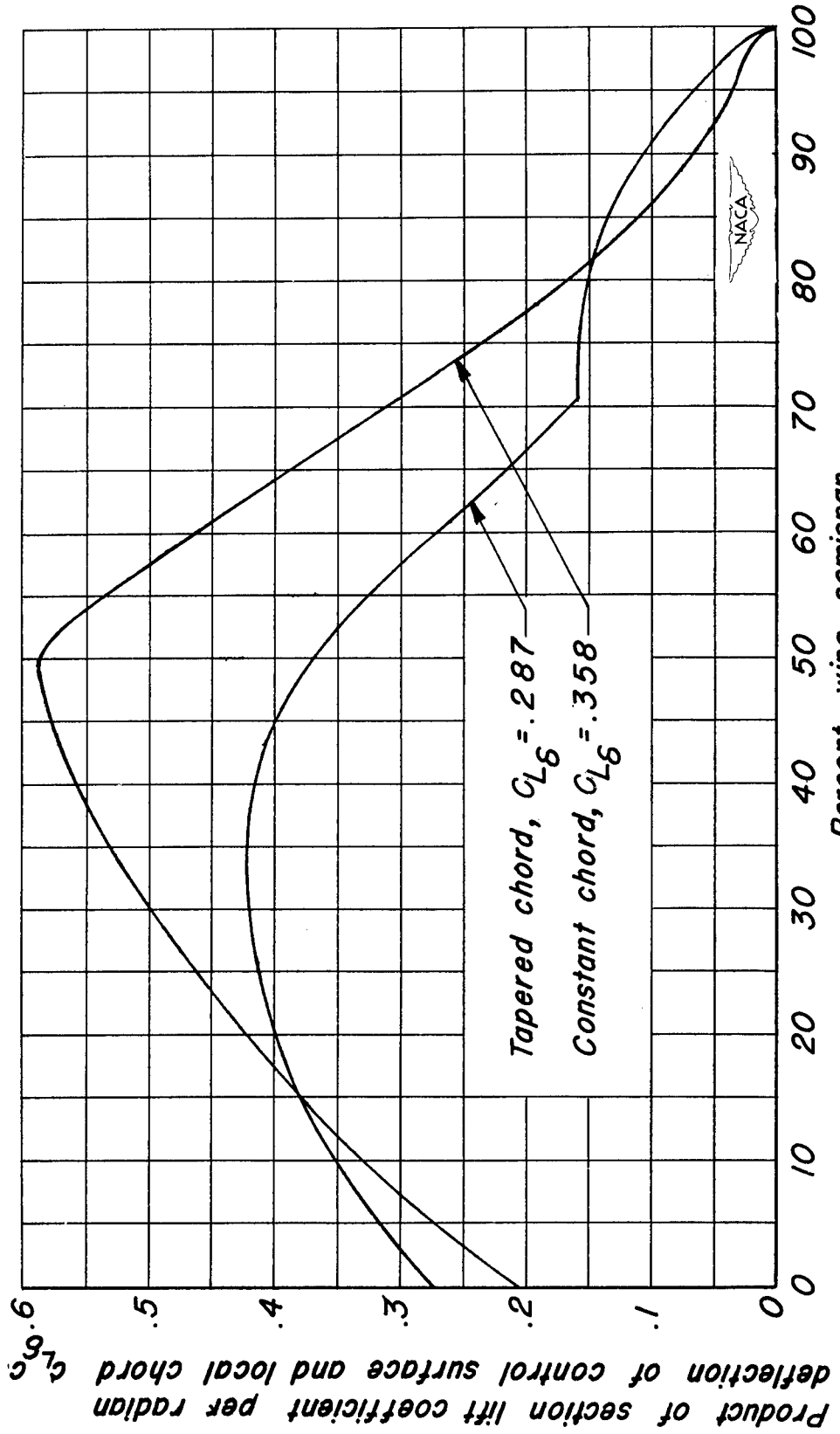

Figure 11.- Spanwise variation of the product of the section value of c_{l_δ} and the local chord for tapered and constant-chord control surfaces with cross - stream tips.

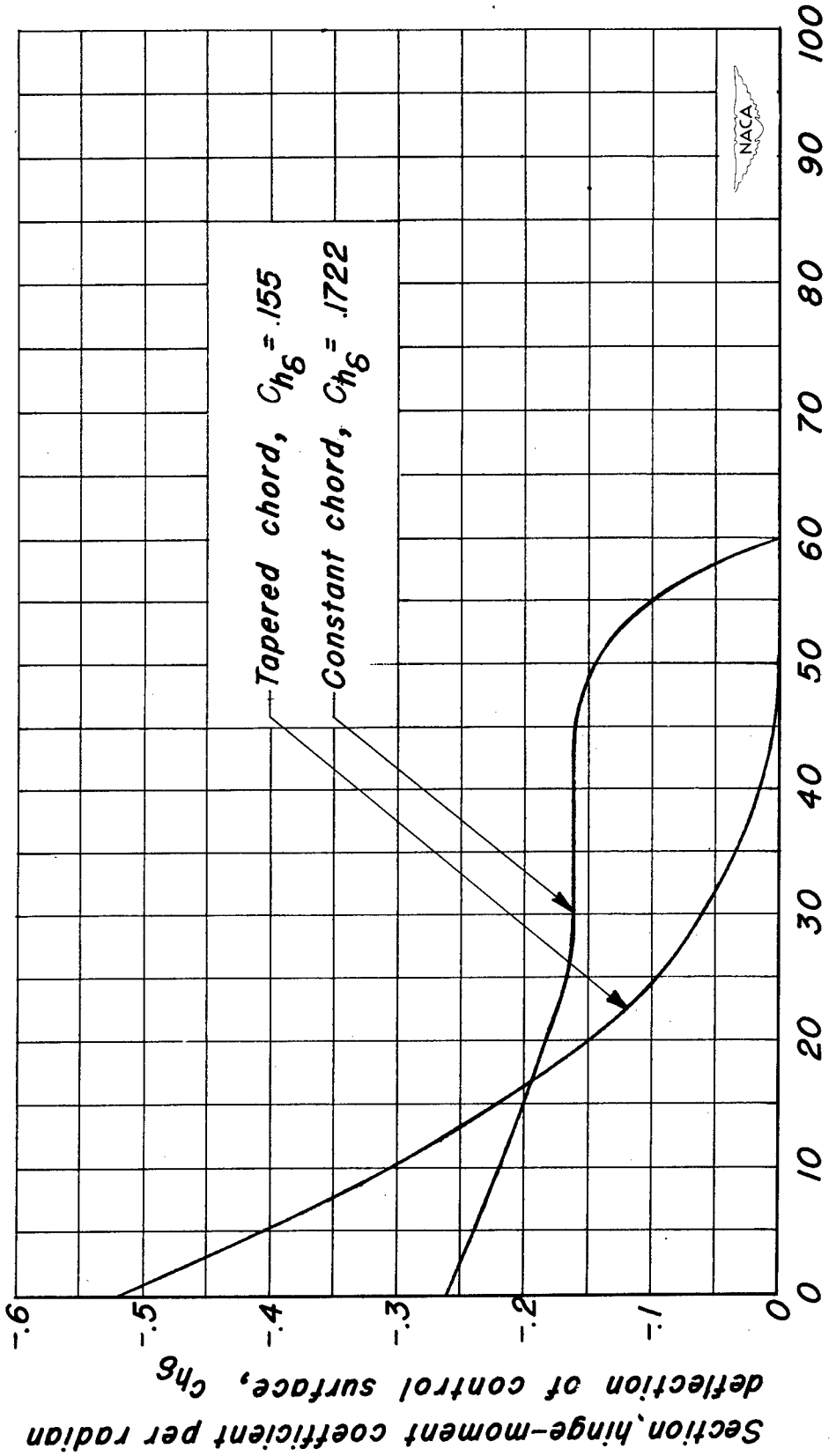

Figure 12.- Spanwise variation of the section value of c_{h_δ} for tapered and constant-chord control surfaces with cross-stream tips.

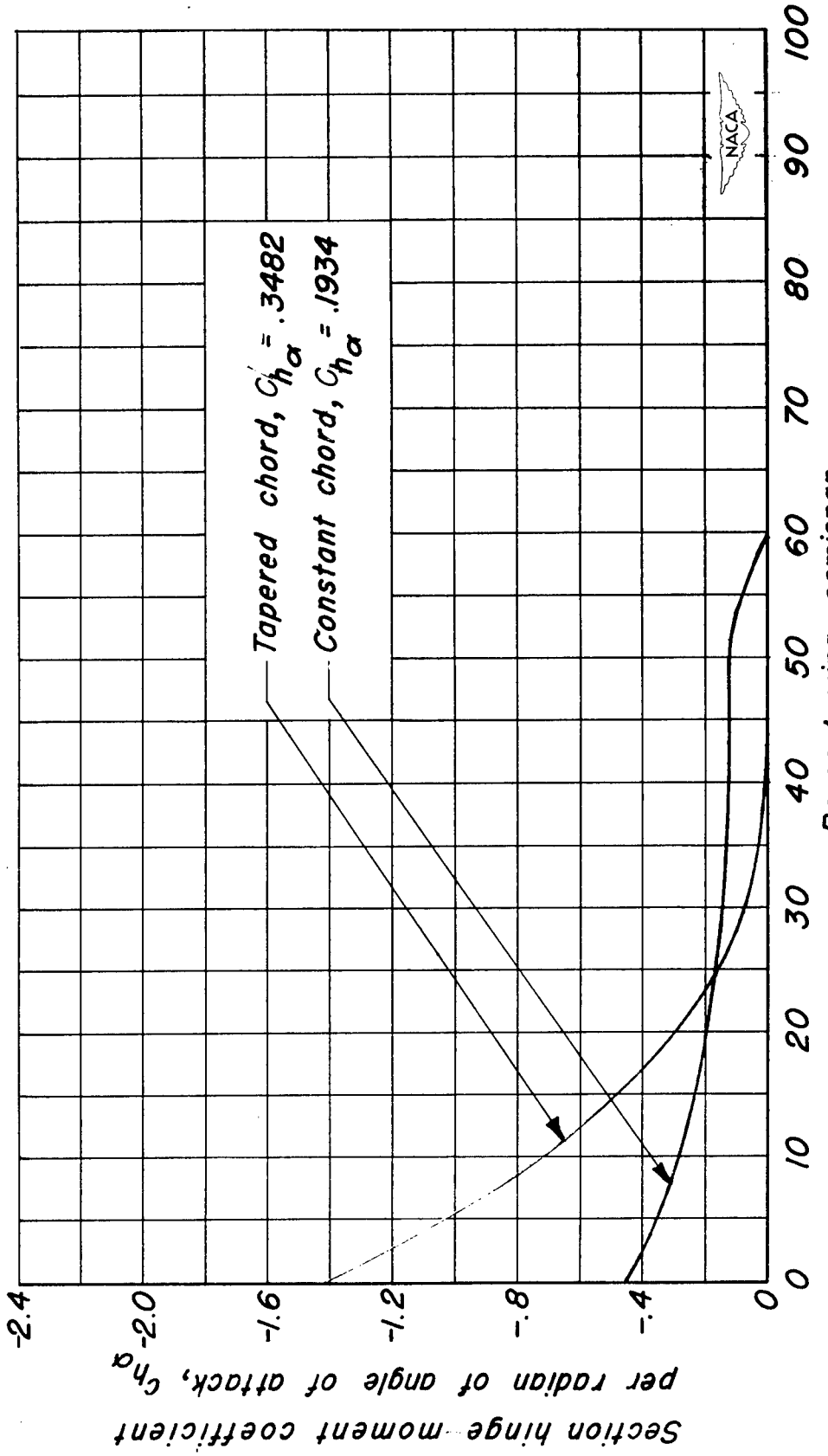

Figure 13.- Spanwise variation of the section value of c_{h_α} for tapered and constant-chord control surfaces with cross-stream tips.

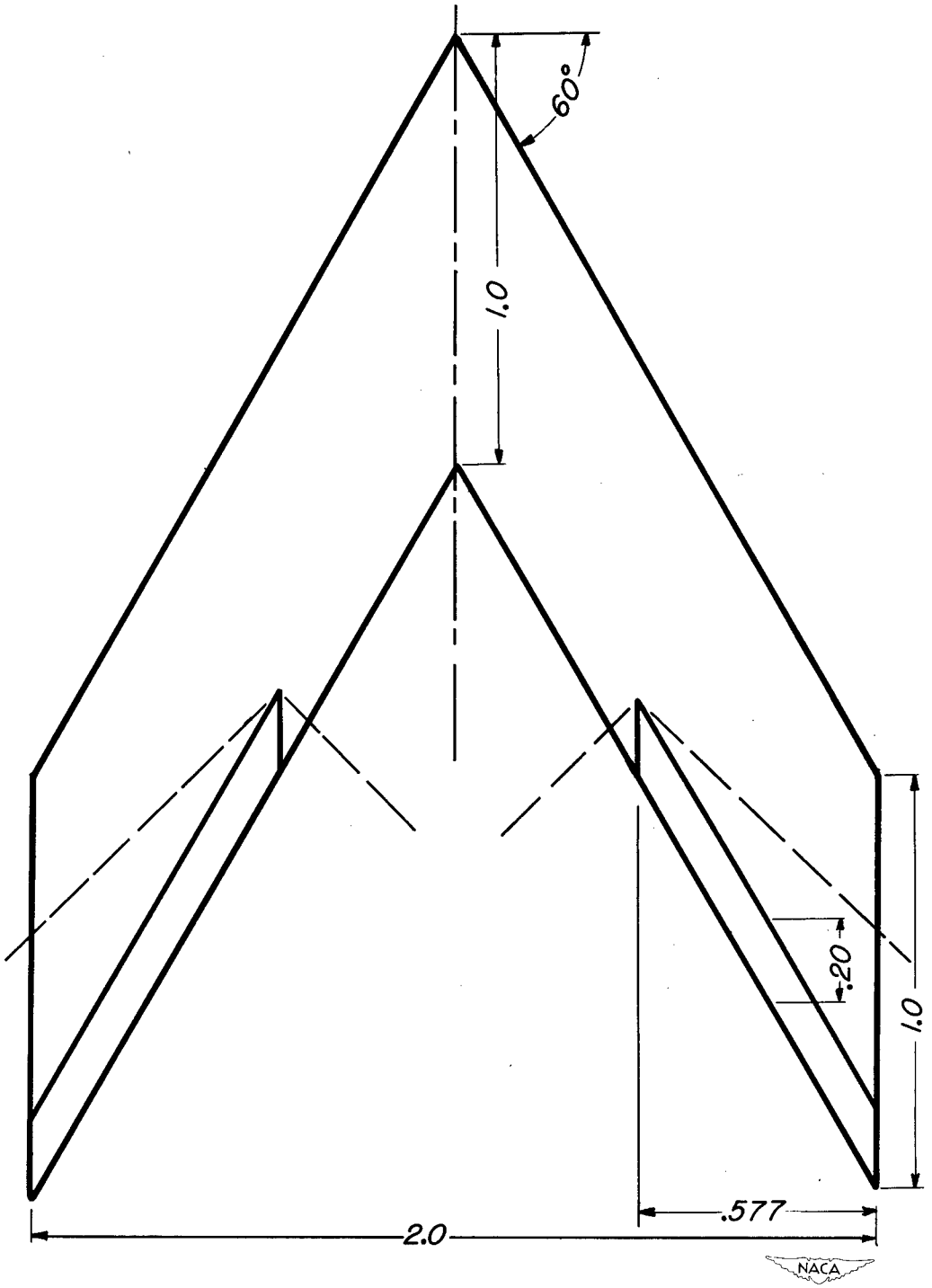

Figure 14.- Lateral control surfaces on an untapered swept-back wing.

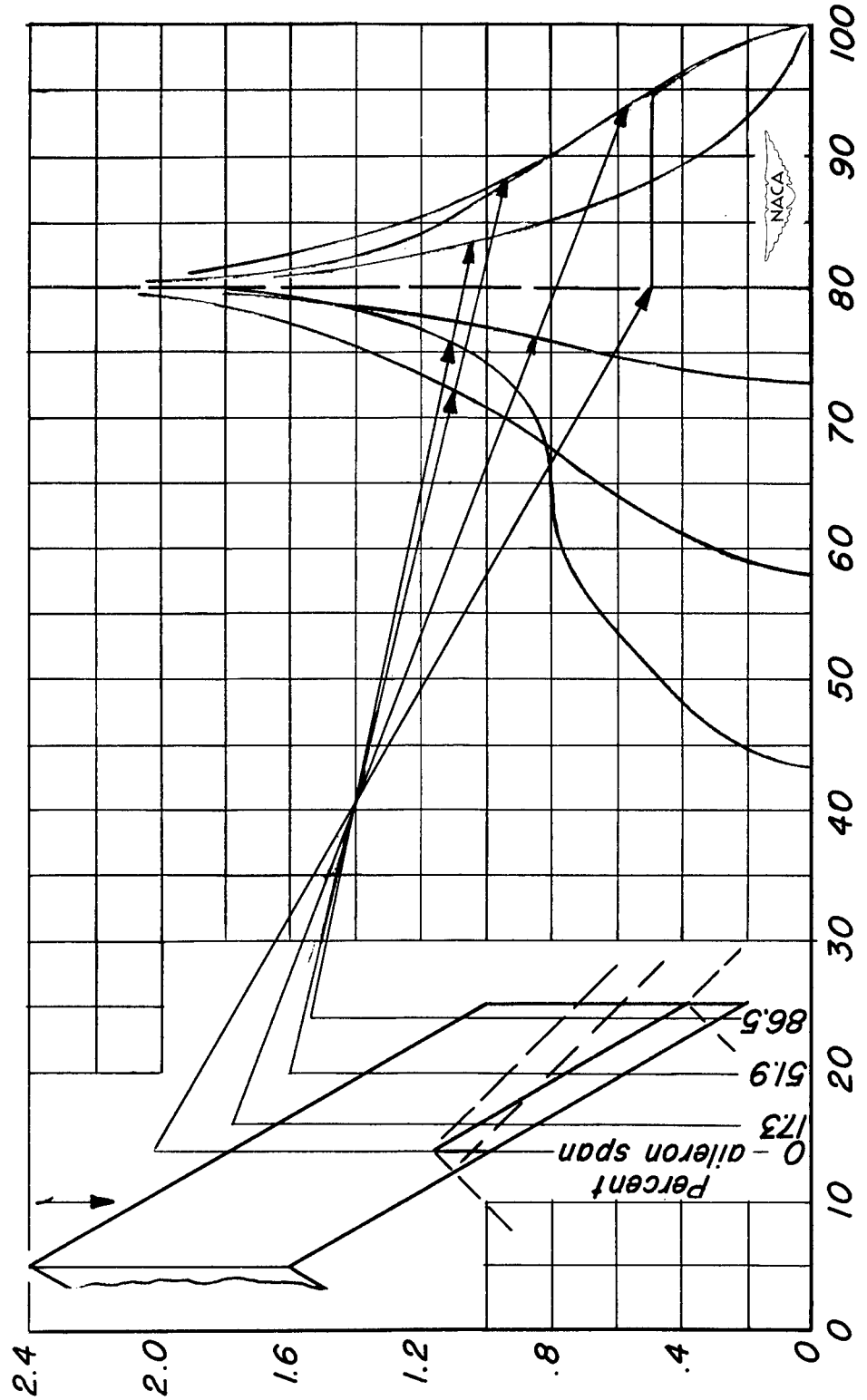

Figure 15.- Chordwise variation of lifting-pressure coefficient at various spanwise stations.

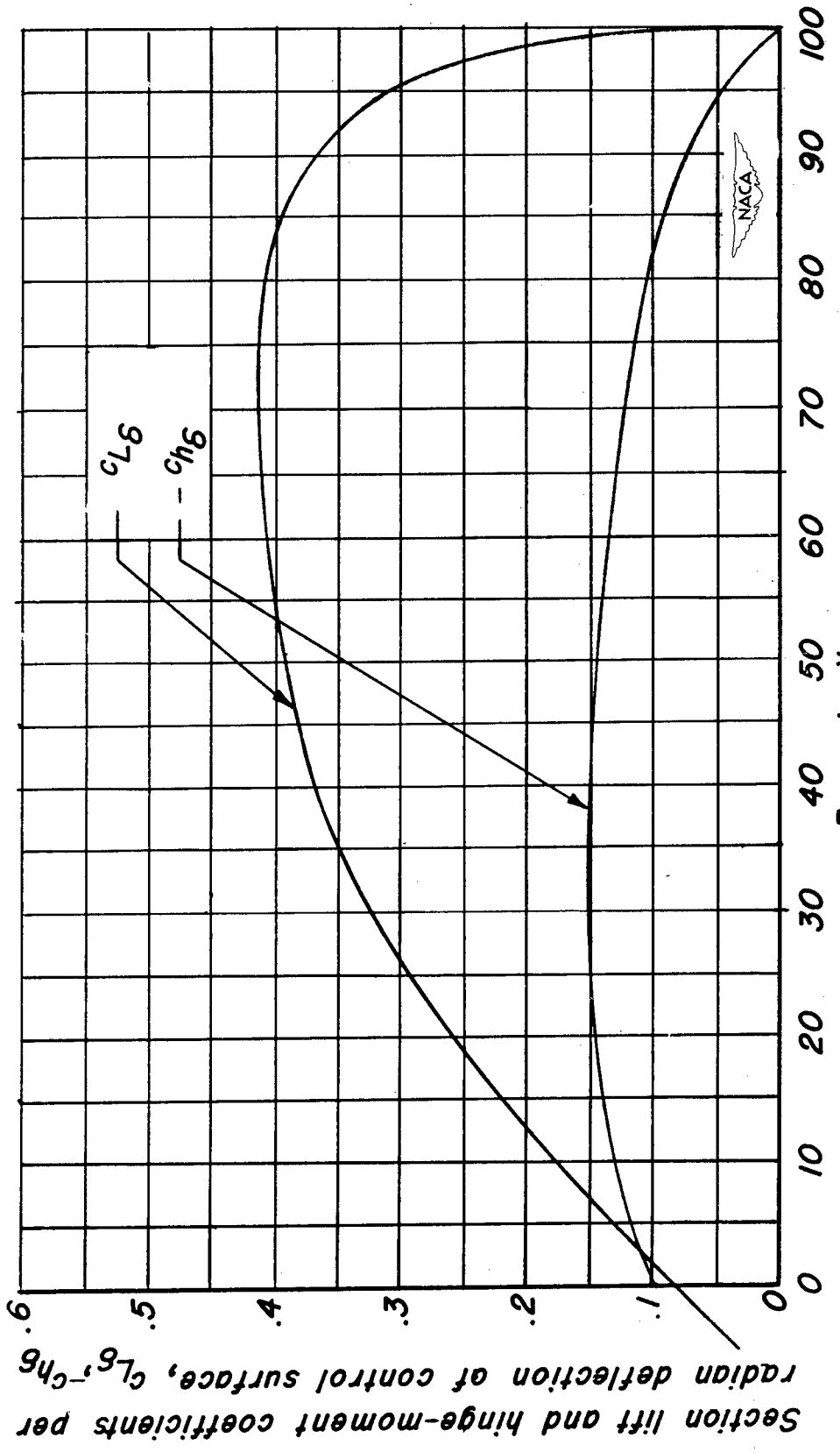

Figure 16.- Variation of the section values of c_{h_δ} and c_{l_δ} along the span of the aileron.